

**INDIGENOUS DESIGN OF PITCH CONTROL SYSTEM OF
SHORT RANGE AIRCRAFT**

by
Nafis Kabir

A thesis submitted to the Department of Electrical and Electronic Engineering in partial
fulfillment of the requirements for the degree
of
MASTER OF SCIENCE IN ELECTRICAL AND ELECTRONIC ENGINEERING



Under the supervision of

Dr. Enamul Basher

Professor

Department of Electrical and Electronic Engineering
Bangladesh University of Engineering and Technology

BANGLADESH UNIVERSITY OF ENGINEERING AND TECHNOLOGY,
DHAKA – 1000, BANGLADESH

September, 2013

The thesis titled “Indigenous Design of Pitch Control System of Short Range Aircraft” submitted by Nafis Kabir, Roll no: 040806104, Session: April, 2008 has been accepted as satisfactory in partial fulfillment of the requirement for the degree of MASTER OF SCIENCE IN ELECTRICAL AND ELECTRONIC ENGINEERING on 28/09/2013.

BOARD OF EXAMINERS

1.

Dr. Enamul Basher
Professor
Department of Electrical and Electronic Engineering
Bangladesh University of Engineering and Technology
(BUET) Chairman

2.

Dr. Pran Kanai Saha
Professor and Head
Department of Electrical and Electronic Engineering
Bangladesh University of Engineering and Technology
(BUET) Member
(Ex-officio)

3.

Dr. Mohammad Jahangir Alam
Professor
Department of Electrical and Electronic Engineering
Bangladesh University of Engineering and Technology
(BUET) Member

5.

Dr. Md. Ashraful Hoque
Professor
Department of Electrical and Electronic Engineering
Islamic University of Technology (IUT)
Board Bazar, Gazipur Member
(External)

CANDIDATE'S DECLARATION

It is hereby declared that this thesis or any part of it has not been submitted elsewhere for the award of any degree or diploma or publication.

Nafis Kabir

Student ID: 040806104

ACKNOWLEDGEMENT

All praises to Allah, the creator of this universe, who gave us the ability to understand a bit of His supreme engineering and herewith extract knowledge from nature to improve our living. This research would not have been possible without His blessing. After that, I would like to express my profound gratitude to my thesis supervisor, Professor Dr. Enamul Basher, for his continuous support and guidance throughout this study. Then I extend my appreciation to my parents and to my wife, who have always been there to support and inspire me. Moreover, I would like to thank my colleagues: Md. Shafiqul Islam, Md. Naquibul Islam, Mirza Masroor Ahmed and Md. Abdullah, from Bangladesh Airlines Training Center, who have shared my official workload to spare me time to continue this thesis work. Finally, I would like to convey my regards to all others who are directly or indirectly related to this thesis by sharing their ideas, suggestions and finally supporting me.

ABSTRACT

In aviation industry, our country all along comprises a group of airlines; operating and maintaining their fleet, residing in the consumer end of the technological flow. Sometimes for a minor off-the-manual modification or repair, we have to remain contained for solution from the concerned foreign manufacturer and hence flights get delayed, even cancelled. So its about time we should initiate designing our own aircrafts, beginning from the modeling in control aspect.

Flight control design is a bit concealed and fairly complex. It depends largely on the type of airplane, it's operating condition, it's airframe, the actuation system, the signal processing system and the sensors that are associated with it. This thesis work confines the subject matter only on pitch control system of short range civil airplane. At first, a prototype of a very basic configuration was built. And then an autopilot was developed for that prototype. Simply in-flight stability was considered here, discarding route planning capability and take-off/landing scenarios. A model describing the dynamics of that prototype was derived using semi empirical method. Based on this model, a Proportional Integral Differential (PID) controller for longitudinal stability was developed. Though practical implementation of this controller did not take place, but it rendered a satisfactory result in real time simulation environment. Finally, cost assessment was done to estimate the feasibility of this design, extending an approximation for a carrier airplane.

TABLE OF CONTENTS

ACKNOWLEDGEMENT	iv
ABSTRACT	v
TABLE OF CONTENTS	vi
LIST OF FIGURES	ix
LIST OF TABLES	xi
NOMENCLATURE	xii
CHAPTER 1: INTRODUCTION	1
1.1 Introduction	1
1.1.1 Datcom+ Pro.....	2
1.1.2 Simulink	3
1.1.3 FlightGear.....	3
1.2 Literature Review	4
1.3 Motivation	5
1.4 Objective of the Thesis.....	6
1.5 Thesis Outline	6
CHAPTER 2: AIRCRAFT AND BASIC AERODYNAMICS	8
2.1 Introduction	8
2.2 Airplane Components.....	8
2.3 Flight Control	9
2.4 Aerodynamic Forces	14
2.5 Airfoil.....	15

CHAPTER 3: AIRPLANE DYNAMICS	19
3.1 Introduction	19
3.2 Coordinate Systems and Forces Acting on Airplane	19
3.3 Derivation of the Equations of Motion	20
3.4 Axis Transformation	24
3.5 Angle of Attack, Sideslip Angle, Flight Path Angle	28
3.6 Stability and Wind Reference Frames	29
3.7 Linearization of Equations of Motion	30
3.8 Equations of Longitudinal Motion	34
3.9 Stability and Control Derivatives for Longitudinal Motion.....	35
CHAPTER 4: THE MODEL UAV – ENA-01	37
4.1 Introduction	37
4.2 ENA-01 Specifications.....	37
CHAPTER 5: THE DESIGN PROCESS	39
5.1 Introduction	39
5.2 ENA-01 Modeling by Datcom+ Pro	40
5.3 Simulink Implementation of ENA-01	44
5.4 Visualization in FlightGear	50
5.5 Microcontroller Code Generation	50
CHAPTER 6: ECONOMIC EVALUATION	52
6.1 Introduction	52
6.2 Cost for Pitch Controller Installation in ENA-01	52

6.3 Estimating Cost for Carrier Airplane	53
CHAPTER 7: CONCLUSION AND SUGGESTION FOR FUTURE WORK	55
7.1 Conclusion.....	55
7.2 Suggestion for Future Work.....	55
APPENDIX I: DATCOM	56
APPENDIX II: Datcom input file (.dcm)	60
Bibliography.....	63
Attached Disk	

LIST OF FIGURES

Figure 2.1: Principal airframe units of Cessna 172	8
Figure 2.2: Control surfaces movement around three axes of flight	10
Figure 2.3: Aileron working principle (looking from aft)	11
Figure 2.4: Elevator working principle	11
Figure 2.5: Rudder working principle	12
Figure 2.6: Flight control surfaces of Boeing 737 airplane	13
Figure 2.7: Forces acting on an airplane in steady state cruise flight	14
Figure 2.8: Force vectors during a stabilized climb	15
Figure 2.9: Generation of lift and drag in an airfoil	15
Figure 2.10: Effect on increasing AOA	16
Figure 2.11: C_L and C_D at various angles of attack	17
Figure 3.1: Body-fixed ($X_b Y_b Z_b$) and Earth-fixed ($X' Y' Z'$) coordinate system	19
Figure 3.2: Definition of vector components in the airplane equations of motion	23
Figure 3.3: Airplane Orientation with Euler Angles	25
Figure 3.4: Illustration of Figure 3.3, rotation sequence from left to right	25
Figure 3.5: Angle of attack (α) and sideslip angle (β)	28
Figure 3.6: Angle of attack (α), sideslip angle (β), pitch angle (θ)	29
Figure 3.7: Stability and wind frame	29
Figure 4.1: ENA-01	37
Figure 5.1: Block diagram of integrated flight dynamics modeling	39
Figure 5.2: A portion of the output file (.out) for ENA-01	41
Figure 5.3: Lift and drag coefficient at different AOA	42
Figure 5.4: ENA-01 airframe in AC3D view (.ac)	43

Figure 5.5: Fuselage cross section at different stations	43
Figure 5.6: Airfoil profiles of wing, horizontal and vertical stabilizer	43
Figure 5.7: Implementing equations of motion	44
Figure 5.8: Force and moment computation	44
Figure 5.9: Calculation of gravity force.....	45
Figure 5.10: Calculation of propulsive force and moment	45
Figure 5.11: Incorporating airplane operating environment	46
Figure 5.12: Actuators of flight control surfaces	46
Figure 5.13: Longitudinal controller- inner pitch loop and outer altitude loop.....	47
Figure 5.14: Autopilot design using PID controller	47
Figure 5.15: A portion of the state space trimmed output	48
Figure 5.16: Tuning of the altitude controller.....	48
Figure 5.17: Altitude command and response	49
Figure 5.18: Altitude command and response with turbulence	49
Figure 5.19: FlightGear data feed setup and visualization	50
Figure 5.20: Generated C code for ‘Autopilot’ subsystem (pitch controller).....	51
Figure 6.1: Proposed onboard components of pitch controller for ENA-01	52

LIST OF TABLES

Table 2.1: Secondary/Auxiliary Flight Control Surfaces	13
Table 4.1: Technical Specifications of ENA-01	38
Table 5.1: Stability and Control Derivatives from Datcom output (for ENA-01).....	42
Table 6.1: Price detail for ENA-01 pitch controller	53
Table 6.2: Price estimation for a manned aircraft.....	54

NOMENCLATURE

L_t	: Lift
D_g	: Drag
C_L	: Coefficient of Lift
C_D	: Coefficient of Drag
\bar{q}_a	: Dynamic Pressure of Air
ρ_a	: Atmospheric Density
V_a	: Relative Velocity of Air
S	: Surface Area of the Wing
C_P	: Coefficient of Parasitic Drag
C_I	: Coefficient of Induced Drag
$X_b Y_b Z_b$: Body Fixed or Non-Inertial Reference Frame
$X'Y'Z'$: Earth Fixed or Inertial Reference Frame
dm	: An Elementary Airplane Mass
\vec{r}	: Position Vector which connects the CG with the Airplane Mass Element
x, y, z	: Components of \vec{r} about $X_b Y_b Z_b$ frame
\vec{r}'	: Position Vector from the origin of $X'Y'Z'$ frame to the Mass Element
x', y', z'	: Components of \vec{r}' about $X'Y'Z'$ frame
\vec{r}'_P	: Position Vector from the origin of $X'Y'Z'$ frame to Airplane CG
\vec{g}	: Gravitational Acceleration along Z' axis
g_x, g_y, g_z	: Gravitational Acceleration Components about $X_b Y_b Z_b$ frame
ρ_A	: Local Mass Density of the Airplane
\vec{F}	: Total Aerodynamic and Thrust Force Per Unit Area
m	: Total Mass of The Airplane

- \vec{V}_P : Velocity of The Airplane
 U, V, W : Airplane Velocity Components about $X_b Y_b Z_b$ frame
 \vec{F}_A : Aerodynamic Force
 F_{Ax}, F_{Ay}, F_{Az} : Aerodynamic Force Components about $X_b Y_b Z_b$ frame
 \vec{F}_T : Thrust Force
 F_{Tx}, F_{Ty}, F_{Tz} : Aerodynamic Moment Components about $X_b Y_b Z_b$ frame
 \vec{M}_A : Aerodynamic Moment
 L_A, M_A, N_A : Aerodynamic Moment Components about $X_b Y_b Z_b$ frame
 \vec{M}_T : Thrust Moment
 L_T, M_T, N_T : Thrust Moment Components about $X_b Y_b Z_b$
 $\vec{\omega}$: Angular Rotation Vector of $X_b Y_b Z_b$ frame relative to $X'Y'Z'$ frame
 P, Q, R : Angular Velocity Components about $X_b Y_b Z_b$ frame
 I_{xx}, I_{yy}, I_{zz} : Airplane Moment of Inertias about $X_b Y_b Z_b$ frame
 I_{xx}, I_{yz}, I_{zx} : Airplane Product of Inertias about $X_b Y_b Z_b$ frame
 Φ : Airplane Roll or Bank Angle
 Θ : Airplane Pitch Angle
 Ψ : Airplane Heading or Yaw Angle
 X : Total Force along X_b axis
 Y : Total Force along Y_b axis
 Z : Total Force along Z_b axis
 L : Total Moment about X_b axis
 M : Total Moment about Y_b axis
 N : Total Moment about Z_b axis
 α : Angle of Attack

β	: Angle of Sideslip
γ	: Flight Path Angle
$X_{ST}Y_{ST}Z_{ST}$: Stability Reference Frame
$X_WY_WZ_W$: Wind Reference Frame
δ_E	: Elevator Deflection
C_m	: Pitching Moment Coefficient
C_N	: Normal Force Coefficient
C_A	: Axial Force Coefficient
$C_{L\alpha}$: Lift Curve Slope (Derivative of Lift Coefficient with respect to angle of attack)
$C_{m\alpha}$: Pitching Moment Curve Slope (derivative of Pitching Moment Coefficient with respect to angle of attack)
$C_{Y\beta}$: Derivative of side-force coefficient with respect to sideslip angle
$C_{l\beta}$: Derivative of rolling-moment coefficient with respect to sideslip angle

CHAPTER 1

INTRODUCTION

1.1 Introduction

A hundred years after the first controlled flight of a manned, heavier-than-air vehicle [1]; we can look back with admiration at the phenomenal progress that has been made in aviation industry [2-3]. In early age, flight control system was a purely mechanical, which connected the control wheel of the pilot directly to the control surfaces of the aircraft by rods, levers, cables and pulleys [3]. The aerodynamic forces on the control surfaces were limited by the physical capabilities of the pilot. Eventually, it phased out with progress in control laws, especially in the area of automation of flight, led to the development of the fly-by-wire system [4-5], power-by-wire system [6] and fly-by-optics system [6-7]. Lately implementation of intelligent, adaptive and reconfigurable flight control systems [8-10] in modern era has ensured more reliable, robust, efficient aircraft operation.

Flight control development research requires flight testing, both for validation of results obtained on the ground, and to guide the research [11]. In general, the more complex the research issues, the more flight testing must be done to get reliable answers. In some cases, such as flight testing involving spins or other out-of-control motion, or developing reconfigurable controls under failure conditions, it is impractical to use manned aircraft for flight research, because of the high cost and safety risks. Since sub-scale flying models, also known as Unmanned Air Vehicle (UAV) are used, as they are less expensive and risks can be taken in research and development that could never be tolerated in a piloted flight test [12]. A UAV can provide increased confidence in the methods and developments before risking the large investment ultimately necessary for a full-scale flight test demonstration [13-14].

Therefore, in this research, to extend the scope of flight control design, up to the

execution level of short range civil aircraft, a UAV, named ENA-01 was constructed. To develop a pitch controller for this ENA-01, a model based approach was embraced. It started from configuring the geometry of the UAV in *Datcom+ Pro*, which is a program that computes static and dynamic stability and control characteristics of fixed wing aircrafts. The output of this program was fed to *Simulink*, with the help of which, the desired controller was designed and optimized. Alongside, *FlightGear*, an open source simulation software was utilized to visualize the simulation in real time environment. Short descriptions of these tools are presented in the later sections.

1.1.1 Datcom+ Pro

The *Datcom+ Pro* program is the outcome of a series of work done in different era. It started as the name *Datcom* [15], which is the United States Air Force Data Compendium, a 3100-page collection of equations used in designing airplanes. This manual dates back to the 1930's-1950's, before computer, when designs and calculations were done by hand and with slide rules.

Digital Datcom [16] is the computer program written in the 1960's-1970's to incorporate many of these techniques into a computer program, to speed the process of analyzing a new or existing aircraft design. The original one is a batch program, written in 60,000+ lines of Fortran IV code, and hence very user-abusive.

Datcom+ [17] was an extension of the Digital Datcom program, which incorporated some tools to make it easier to use the base program.

Datcom+ Pro [17] is the next generation of this program, which has been made much more user-friendly. Visualization tools allow us to see the aircraft immediately, and coefficient data generated by the program is plotted on graphs for ease of interpretation and inclusion into reports.

All these versions, generally known as Datcom, have incorporated a great deal in cost

reduction and speeding up the aircraft designing process by eliminating Computational Fluid Dynamics (CFD) analysis and wind tunnel test [18-21] . More detail of this program, it's input, output, routine and limitation are described in Appendix I.

1.1.2 Simulink

Simulink [22] is an interactive tool for modeling, simulating, and analyzing dynamic systems. It is integrated with *MatLab*, and developed by the same *MathWorks*. Its primary interface is a graphical block diagramming tool and a customizable set of block libraries. Simulink is widely used in control theory for multi-domain simulation and model based design [23]. There are different toolboxes defined in the library which can be used readily to design any control system of any vehicle.

Aerospace Blockset [24] software extends Simulink with blocks for modeling and simulating aircraft, spacecraft, rocket, and propulsion systems, as well as UAV. It also includes blocks that implement mathematical representations from aerospace standards, common references, and first principles. Blocks for modeling equations of motion and for navigation, gain scheduling, visualization, unit conversion, and other key operations are also provided. It also has code generation support.

1.1.3 FlightGear

FlightGear [25] flight simulator is a free, open source multi-platform flight simulator. It has specific builds for a variety of operating systems including Microsoft Windows, Mac OS X, Linux, IRIX, and Solaris. FlightGear code is released under the terms of the GNU General Public License; hence it is a free software [26].

FlightGear has hundreds of aircraft and Flight Dynamics Model (FDM), which uses one of these three main data models - JSBSim, YAsim, or UIUC. OpenGL is used for its integrated 3D graphics routines and have several networking option to support multiplayer protocol [25].

Aerospace Blockset has a sub-library named *Animation* to interface a Simulink model directly to FlightGear. This enables us to directly see the changes in aircraft attitude when there is a change in model, control or input parameter. Therefore now-a-days, it has become a common practice to use this kind of simulator before actual flight testing [27-28].

1.2 Literature Review

For being an Engineering Instructor in the Avionics Faculty of Bangladesh Airlines Training Center, I have gathered a lot of knowledge about aircraft maintenance. The hands-on experience in line and base maintenance of the fleet helped me to get a better understanding of the operations of different aircraft systems. In basic Aircraft Maintenance Engineering (AME) training, the universal books that are used as reference are Federal Aviation Administration (FAA) publications [29] and European Aviation Safety Agency (EASA) publications [30]. Other supporting material for building up knowledge on dynamics of flight, aircraft electrical system, instrument system and communication and navigation system are from [31-37]. Another important contribution is from the manuals that were provided by manufacturers with the aircrafts such as Aircraft Maintenance Manual (AMM), Wiring Diagram Manual (WDM), Troubleshooting Manual (TSM), Fault Isolation Manual (FIM) etc.

In Chapter 2, some of the definitions and figures on aircraft and basic aerodynamics are taken from [38-39]. This chapter gives a general idea of the terminologies used in aviation sector without any complex formula. In the subsequent chapter, a detail derivation of the airplane dynamics is placed, which is mostly taken from [40]. This is perhaps the most apprehensible of all the aeronautical engineering books and widely used in all around the world. Some concepts are also extracted from National Aeronautics and Space Administration (NASA) reference publications [41-42]. To understand about automatic

flight control, a great help was [43]. For the theoretical background in control engineering, help was taken from [44-46].

Journals and conference proceedings of the American Institute of Aeronautics and Astronautics (AIAA) and Institute of Electrical and Electronics Engineers (IEEE) were extremely accommodating in constituting the Simulink model. A few of them are listed in the Bibliography section.

Moreover, a great assistance to follow through the whole design process were blogs, groups and discussions boards about Datcom, MathWorks, Simulink, FlightGear. Different web stores and their representatives were helpful to buy and look through the devices that have been recommended for the intended pitch controller.

Nonetheless, this research work would not have been possible without the help of MathWorks technical publications, articles, webinars and constant support from MatLab documentations.

1.3 Motivation

As an individual related to aircraft maintenance, I always have been curious about the design excellence of airplane control. Autopilot and automatic flight control system in modern airplanes have reduced the workload of the pilot in a great extent and it is quite amazing how many flight configuration and operational phenomena are considered for that kind of design. In my classes, often there were questions about the background of autopilot operation and that motivated me to explore the engineering side of it. Moreover, I always wanted to make my own airplane. My supervisor gave me a lot of inspiration to take this challenge. There are some other factors that motivated me. In aviation manufacturing industry, our country has no contribution; not even in the field of UAV research. Our operators often have faced numerous problems to maintain their fleet as we do not have

enough knowledge about the design philosophy and all available options to dispatch an unscheduled maintenance work. Sometimes because of an emergency, like when an aircraft is declared on ground (AOG), we often have to buy components in far higher prices than usual, especially when it is in outstation. And sooner or later, to catch up with the technological advancement in aviation, I felt that this sort of research should commence in our country and I wished to be a part of it.

1.4 Objective of the Thesis

As the title of this thesis indicates, the main objective of this research is to develop a controller for an aircraft in pitch plane. This can be segregated in the following manner

- i. Construct a UAV as an airplane prototype.
- ii. Analyze the characteristics of that UAV.
- iii. Create the longitudinal dynamics model of the UAV in Simulink.
- iv. Develop a controller for that dynamics model.
- v. Assess economic feasibility of the design.

1.5 Thesis Outline

The organization of this thesis is placed below in accordance with the chapter follow through.

Chapter 1: In this chapter, an overview of the thesis is placed with literature review, motivation and objective.

Chapter 2: This chapter presents a general idea about airplane terminologies and basic aerodynamics. It covers the identification and function of different airplane parts, it's attitude

changing mechanism using flight control surfaces, the forces acting on an airplane and how these forces can be controlled.

Chapter 3: In this chapter, dynamics equations for decoupled longitudinal motion of an airplane are derived. It deals with setting up the reference frames and defining motion vectors, then axis transformation producing kinematics and dynamics equation and finally linearization of these equations about steady state conditions.

Chapter 4: This chapter gives a description of the UAV into which the pitch controller would be implemented.

Chapter 5: In this chapter, the development process of the pitch controller is explained. At first, Datcom is used to calculate stability and control derivatives of the UAV. Then these derivatives are fed to a Simulink model where PID controllers are set and tuned considering the effect of environment, gravity, turbulence. The chapter ends with FlightGear visualization and microcontroller code generation process.

Chapter 6: This chapter includes with the economic evaluation of the controller that has been developed for the UAV and cost approximation for a carrier airplane.

Chapter 7: The last chapter draws a conclusion of the thesis and gives suggestion for future scope.

CHAPTER 2

AIRCRAFT AND BASIC AERODYNAMICS

2.1 Introduction

An *aircraft* is a device that is used for flight in the air. Major categories of aircraft are fixed wing aircraft, rotorcraft, glider, and lighter-than-air vehicles. Fixed wing aircraft is the one that is extensively used for passenger carrying civil operation and generally known as airplane. A general description of the structure of an airplane is provided in the following section. Most of the topics of this chapter are taken from [38] and [39].

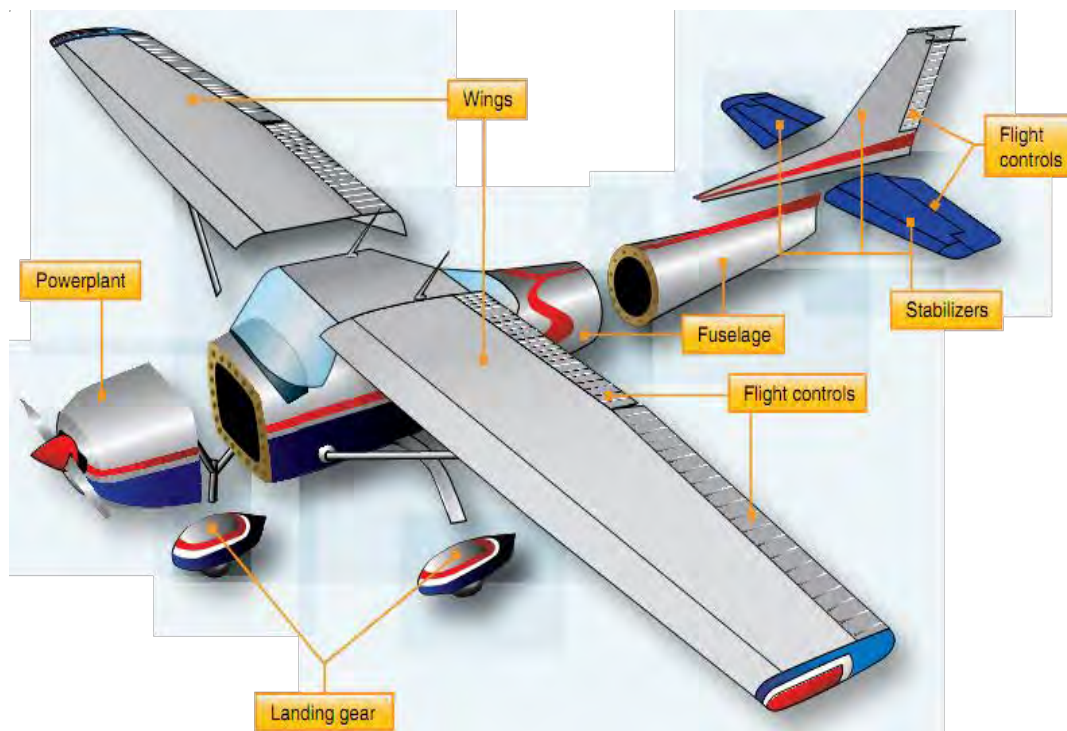


Figure 2.1: Principal airframe units of Cessna 172 [38]

2.2 Airplane Components

As the name implies, the wings of fixed wing aircrafts are attached to the fuselage and are not intended to move independently in a fashion that results in the creation of lift. The airframe of a fixed-wing aircraft consists of these principal units: fuselage, powerplant, wing, stabilizers, landing gear and flight control surfaces, as shown in Figure 2.1.

The *fuselage* is the central body and designed to accommodate the crew, passengers,

and cargo. It also provides the structural connection for the wings and tail assembly.

An aircraft *powerplant* or engine produces thrust to propel an aircraft. Reciprocating engines and turboprop engines work in combination with a propeller to produce thrust. Turbojet and turbofan engines produce thrust by increasing the velocity of air flowing through the engine. All of these powerplants also drive the various systems that support the operation of an aircraft.

The *wings* are airfoils attached to each side of the fuselage and are the main lifting surfaces that support the airplane in flight. At the trailing edge, there are flaps, which are the main lift augmentation device of the airplane. There are numerous wing designs, sizes, and shapes used by the various manufacturers. Each fulfills a certain need with respect to the expected performance for the particular airplane.

The *stabilizers* (both horizontal and vertical) are located in the tail assembly or empennage and assist the airplane to maintain desired stability and control. They accommodate some flight control surfaces.

The *landing gear* is the principal support of the airplane when parked, taxiing, taking off, or landing. The most common type of landing gear consists of wheels, but airplanes can also be equipped with floats for water operations, or skis for landing on snow.

2.3 Flight Control

The control of a fixed-wing aircraft takes place around the lateral, longitudinal, and vertical axes by means of flight control surfaces designed to create movement about these axes. These control devices are hinged or movable surfaces through which the attitude of an aircraft is controlled during takeoff, flight, and landing. They are usually divided into: primary or main flight control surfaces and secondary or auxiliary control surfaces.

The *primary flight control* surfaces on an airplane include: ailerons, elevators, and

rudder. The ailerons are attached to the trailing edge of both wings and when moved, rotate the aircraft around the longitudinal axis. The elevator is attached to the trailing edge of the horizontal stabilizer. When it is moved, it alters aircraft pitch, which is the attitude about the horizontal or lateral axis. The rudder is hinged to the trailing edge of the vertical stabilizer. When the rudder changes position, the aircraft rotates about the vertical axis (yaw). Figure 2.2 shows the movement they create relative to the three axes of flight.

The pilot's command to maneuver the airplane by the control wheel and control stick is transmitted from the cockpit to the actual control surface in a variety of ways depending on the aircraft. A system of control cables and pulleys, push-pull tubes, hydraulics, electric, or a combination of these can be employed.

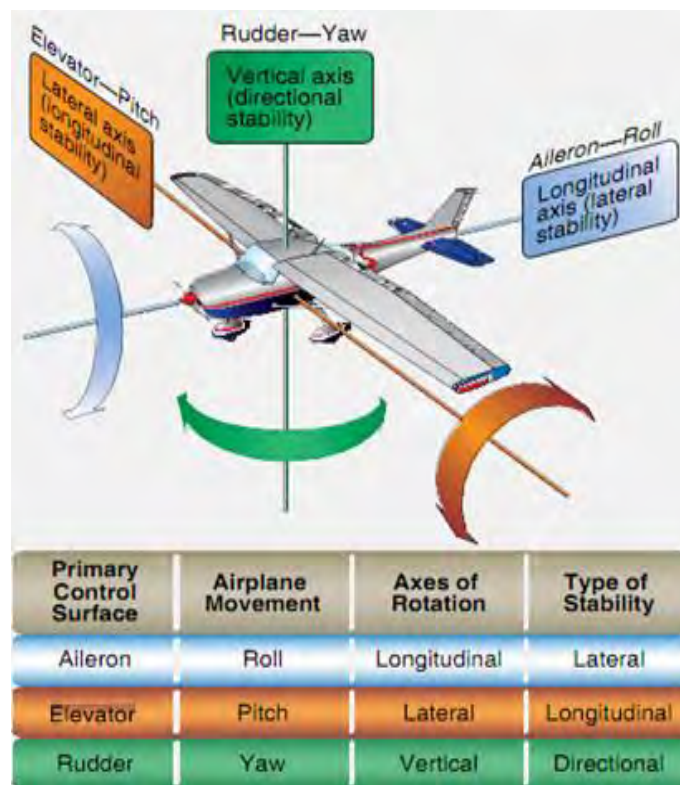


Figure 2.2: Control surfaces movement around three axes of flight [38]

Ailerons control roll about the longitudinal axis. The ailerons are attached to the outboard trailing edge of each wing and move in the opposite direction from each other. Moving the control wheel in the cockpit to the right causes the right aileron to deflect

upward and the left aileron to deflect downward, as shown in Figure 2.3. The upward deflection of the right aileron decreases the camber resulting in decreased lift on the right wing. The corresponding downward deflection of the left aileron increases the camber resulting in increased lift on the left wing. Thus, the increased lift on the left wing and the decreased lift on the right wing causes the airplane to roll to the right.



Figure 2.3: Aileron working principle (looking from aft) [39]

The *elevator* is the primary flight control surface that moves the aircraft around the horizontal or lateral axis. This causes the nose of the aircraft to pitch up or down. The elevator is hinged to the trailing edge of the horizontal stabilizer and typically spans most or all of its width. It is controlled by pushing or pulling the control yoke forward or aft.

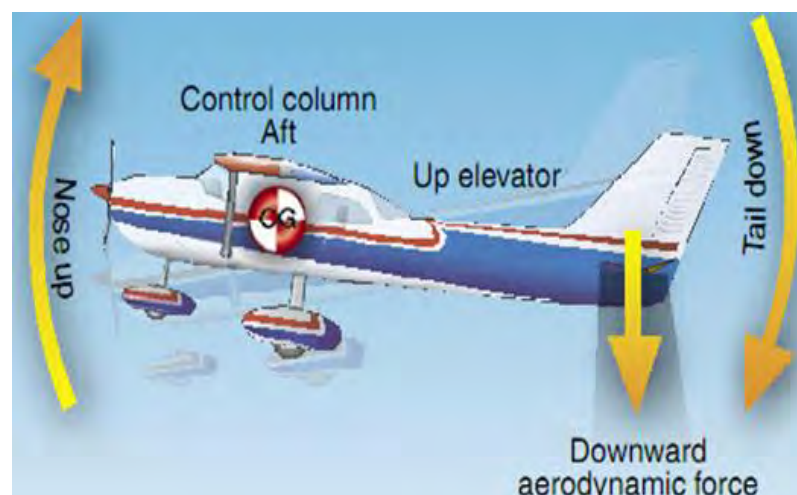


Figure 2.4: Elevator working principle [39]

Aft movement of the control column deflects the trailing edge of the elevator surface

up. This is usually referred to as ‘up’ elevator. The up-elevator position decreases the camber of the elevator and creates a downward aerodynamic force, which is greater than the normal tail-down force that exists in straight-and-level flight. The overall effect causes the tail of the aircraft to move down and the nose to pitch up (Figure 2.4). The pitching moment occurs about the center of gravity (CG). And it’s strength is determined by the distance between the CG and the horizontal tail surface, as well as by the aerodynamic effectiveness of the horizontal tail surface. Moving the control column forward has the opposite effect. In this case, elevator camber increases, creating more lift (less tail-down force) on the horizontal stabilizer/elevator. This moves the tail upward and pitches the nose down.

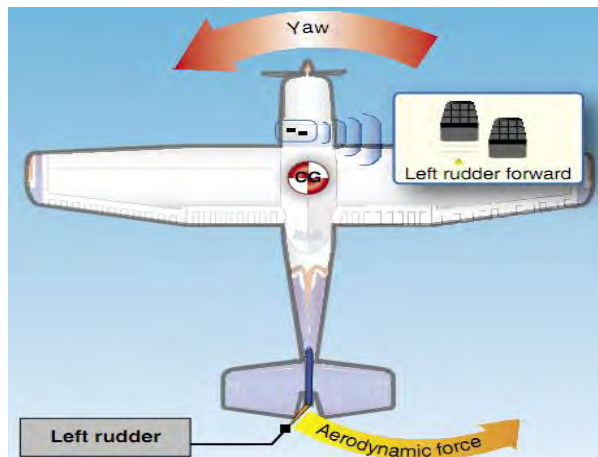


Figure 2.5: Rudder working principle [39]

The *rudder* causes an aircraft to yaw or move about the vertical axis. This provides directional control and thus points the nose of the aircraft in the direction desired. Most aircraft have a single rudder hinged to the trailing edge of the vertical stabilizer. It is controlled by a pair of foot-operated rudder pedals in the cockpit. When the left pedal is pushed forward, the rudder is deflected left into the airflow. Therefore, a horizontal force is exerted in the opposite direction, as shown in Figure 2.5. This alters the airflow around the vertical stabilizer/rudder, and creates a sideward lift that moves the tail to the right and yaws the nose of the airplane to the left.

The following Table gives a basic idea about *secondary flight control surfaces*, with

their positions in the airframe and uses.

Table 2.1: Secondary/Auxiliary Flight Control Surfaces

Name	Location	Function
Flaps	Inboard trailing edge of wings	Extends the camber of the wing for greater lift and slower flight. Allows control at low speeds for short field takeoffs and landings.
Trim tabs	Trailing edge of primary flight control surfaces	Reduces the force needed to move a primary control surface.
Balance tabs	Trailing edge of primary flight control surfaces	Reduces the force needed to move a primary control surface.
Anti-balance tabs	Trailing edge of primary flight control surfaces	Increases feel and effectiveness of primary control surface.
Servo tabs	Trailing edge of primary flight control surfaces	Assists or provides the force for moving a primary flight control.
Spoilers	Upper and/or trailing edge of wing	Decreases (spoils) lift. Can augment aileron function.
Slats	Mid to outboard leading edge of wing	Extends the camber of the wing for greater lift and slower flight. Allows control at low speeds for short field takeoffs and landings.
Slots	Outer leading edge of wing forward of ailerons	Directs air over upper surface of wing during high angle of attack. Lowers stall speed and provides control during slow flight.
Leading edge flap	Inboard leading edge of wing	Extends the camber of the wing for greater lift and slower flight. Allows control at low speeds for short field takeoffs and landings.

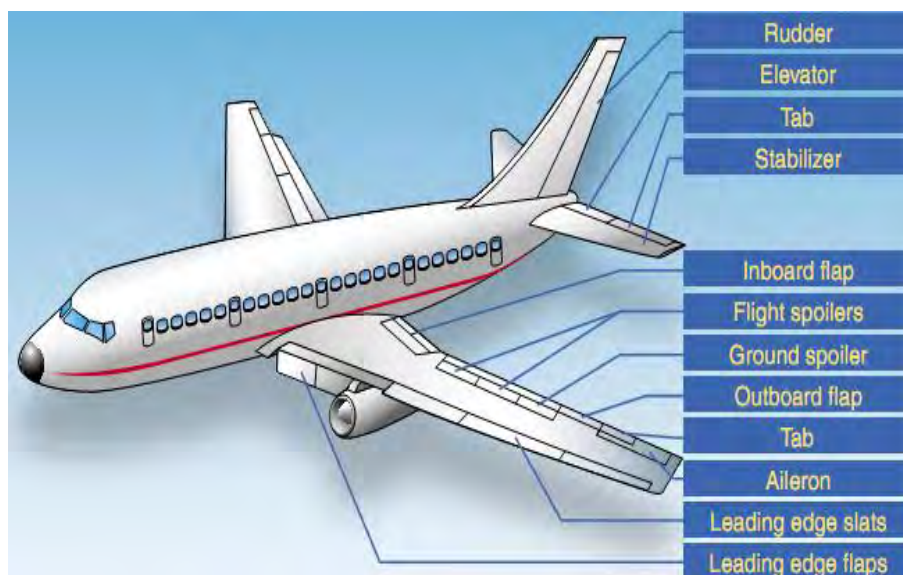


Figure 2.6: Flight control surfaces of Boeing 737 airplane [38]

2.4 Aerodynamic Forces

The forces act on an aircraft are thrust, drag, lift, and weight. They are defined as follows:

- i. Thrust is the forward force produced by the engine by burning fuel. It opposes or overcomes the force of drag and acts parallel to the longitudinal axis.
- ii. Drag is a rearward, retarding force caused by disruption of airflow by the wing, rotor, fuselage, and other protruding objects. Drag opposes thrust, and acts rearward parallel to the relative wind.
- iii. Weight is the combined load of the aircraft itself, the crew, the fuel, and the cargo or baggage. Weight pulls the aircraft downward because of the force of gravity. It opposes lift, and acts vertically downward through the aircraft's center of gravity (CG).
- iv. Lift opposes the downward force of weight, is produced by the dynamic effect of the air acting on the airfoil, and acts perpendicular to the flightpath through the center of pressure (CP).

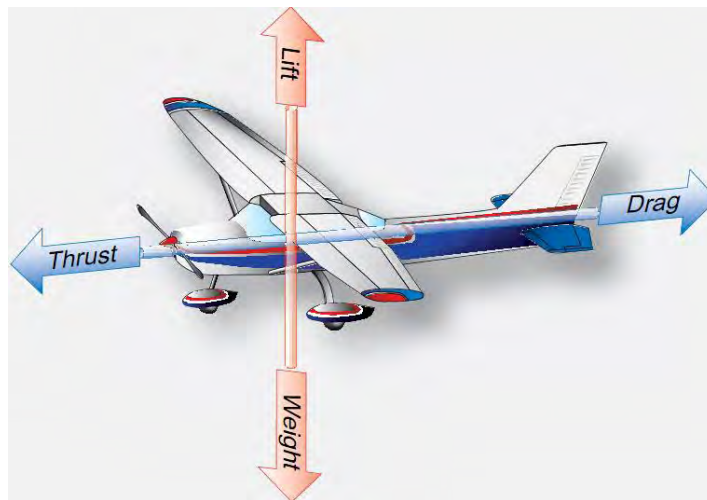


Figure 2.7: Forces acting on an airplane in steady state cruise flight [38]

In steady state cruise flight condition, the sum of the opposing forces is always zero, which means thrust equals drag and lift equals weight. Figure 2.8 shows an airplane in a climbing situation, a portion of thrust is directed upward in climbs and acts as if it were lift

while a portion of weight is directed backward and acts as if it were drag.

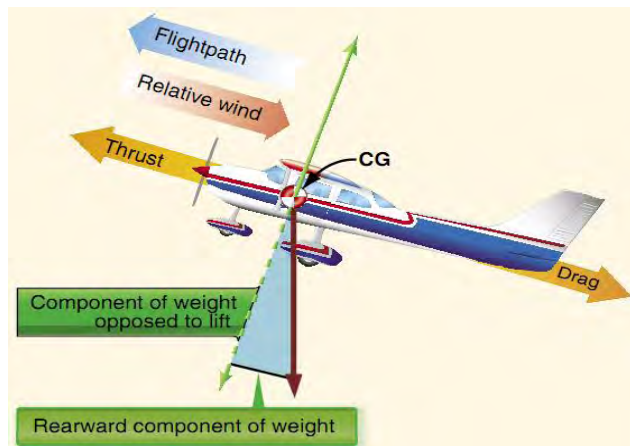


Figure 2.8: Force vectors during a stabilized climb [38]

2.5 Airfoil

Wing of an airplane takes charge in ascending the whole structure because of its airfoil shape. Lift and drag come in as the output of the reaction from the aircraft geometry and relative airflow gained from the forward movement due to thrust. Lift force, in simple words, is generated by differential pressure on upper and lower side of the airfoil or wing. When an airfoil is located in an airstream, the flow divides at the leading edge, the stagnation point. The camber of the airfoil section intends that the air passing over the top surface has further to travel to reach the trailing edge than that travelling along the lower surface. In accordance with Bernoulli's equation the higher velocity along the upper airfoil surface results in a lower pressure, producing a lift force. Figure 2.9 shows the cross section of an airfoil.

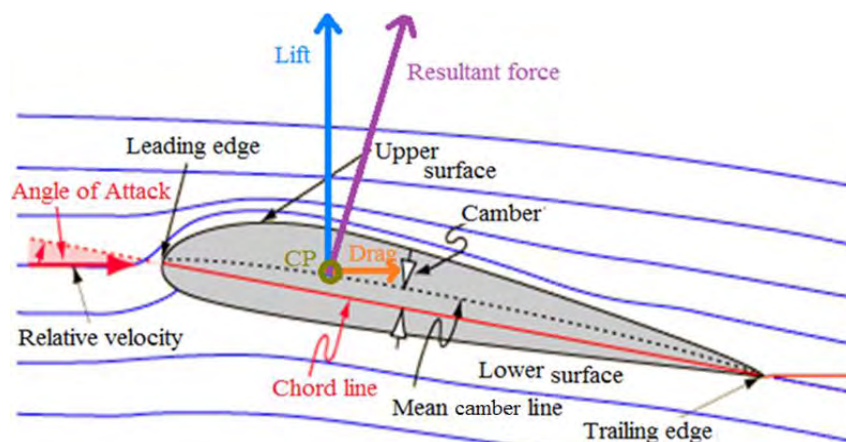


Figure 2.9: Generation of lift and drag in an airfoil

The camber of the airfoil can be controlled by extending and contracting flaps, which evidently changes the angle of attack (AOA) i.e. the angle between the chord line and relative airflow. In fact, aerodynamic forces and airplane stability are direct dependent of AOA in a significant manner. For all positive AOA, the Center of Pressure (CP) moves forward as the pitching angle is increased, until the stall angle is reached after which it suddenly moves backward along the chord line, as shown in Figure 2.10.

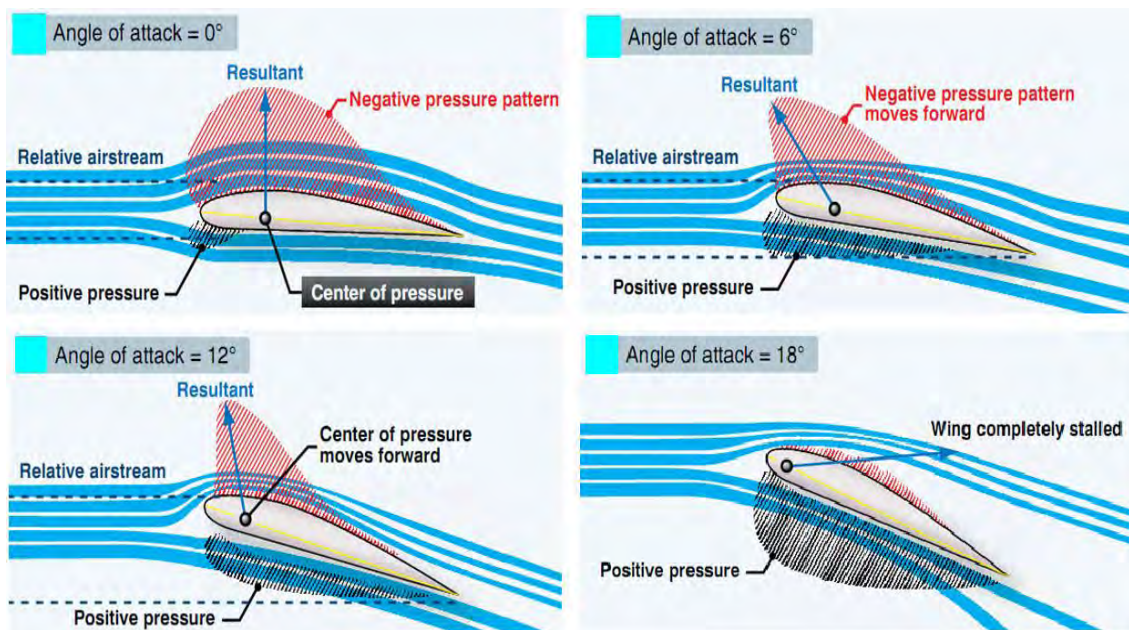


Figure 2.10: Effect on increasing AOA [38]

As we know, drag is the force that resists movement of an aircraft through the air. There are two basic types: parasite drag and induced drag. Parasite drag is the outcome of the displacement of air by the aircraft, turbulence generated in the airstream, or a hindrance of air moving over the surface of the aircraft and airfoil. Induced drag results from the differential pressure acting on the top and bottom surface of the wing, through the wing tip, causing whirlpool action. In a same way as lift increases with increase of AOA, so too does induced drag.

Therefore, to some extent, drag is the price paid to obtain lift. The lift to drag ratio (L_t/D_g) is the amount of lift generated by a wing or airfoil compared to its drag. Hence it indicates airfoil efficiency.

Mathematically, lift and drag can be expressed as

$$L_t = \bar{q}_a S C_L = \left(\frac{1}{2} \rho_a V_a^2\right) S C_L \quad (2.1)$$

$$D_g = \bar{q}_a S C_D = \left(\frac{1}{2} \rho_a V_a^2\right) S C_D \quad (2.2)$$

$$\bar{q}_a = \frac{1}{2} \rho_a V_a^2 \quad (2.3)$$

Where \bar{q}_a = dynamic pressure of air
 ρ_a = atmospheric density (a function of height)
 V_a = relative velocity of air
 S = wing area
 C_L = coefficient of lift
 C_D = coefficient of drag

The above formulas represent the coefficient of lift (C_L) and the coefficient of drag (C_D) respectively. The shape of an airfoil and other lift producing devices (i.e., flaps) effect the production of lift and alter with changes in the AOA.

In unaccelerated flight with the lift and drag data steady, this proportion of C_L/C_D , as well as Lift/Drag can be calculated for specific AOA, as shown in Figure 2.11.

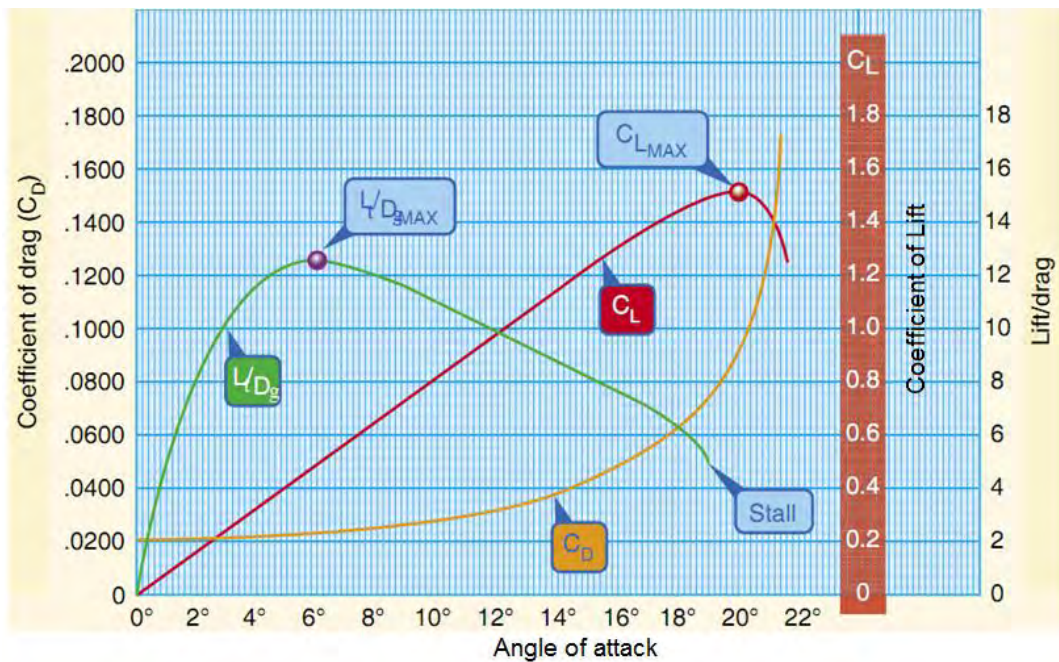


Figure 2.11: C_L and C_D at various angles of attack [39]

Notice in Figure 2.11 that the lift curve reaches its maximum for this particular wing section at 20° AOA, and then rapidly decreases; therefore 20° AOA is the stalling angle. The drag curve increases very rapidly from 14° AOA and completely overcomes the lift curve at 21° AOA. The lift/drag ratio (green) reaches its maximum at 6° AOA, meaning that at this angle, the most lift is obtained for the least amount of drag.

As drag is dependent on lift, it is experimentally found that the coefficients are related in the following manner

$$C_D = C_p + C_l = C_p + KC_L^2 \quad (2.4)$$

Where, C_p and C_l are the contributions from parasitic and induced drag, and the later one is dependent on the coefficient of lift in a quadratic manner.

CHAPTER 3

AIRPLANE DYNAMICS

3.1 Introduction

To design the control system for an aircraft, it is paramount to understand its dynamics and kinematics. In this chapter, the equations of motion of an airplane is deduced and then linked down to decoupled longitudinal dynamics.

3.2 Coordinate Systems and Forces Acting on Airplane

The two major reference frames used in flight dynamics are the body fixed reference frame ($X_b Y_b Z_b$) and the earth fixed or inertial reference frame ($X' Y' Z'$). Supposedly, in latter, Newton's law of motion is considered valid. This means that the rotational velocity of the earth is neglected and it is found acceptable up to hypersonic airplane.

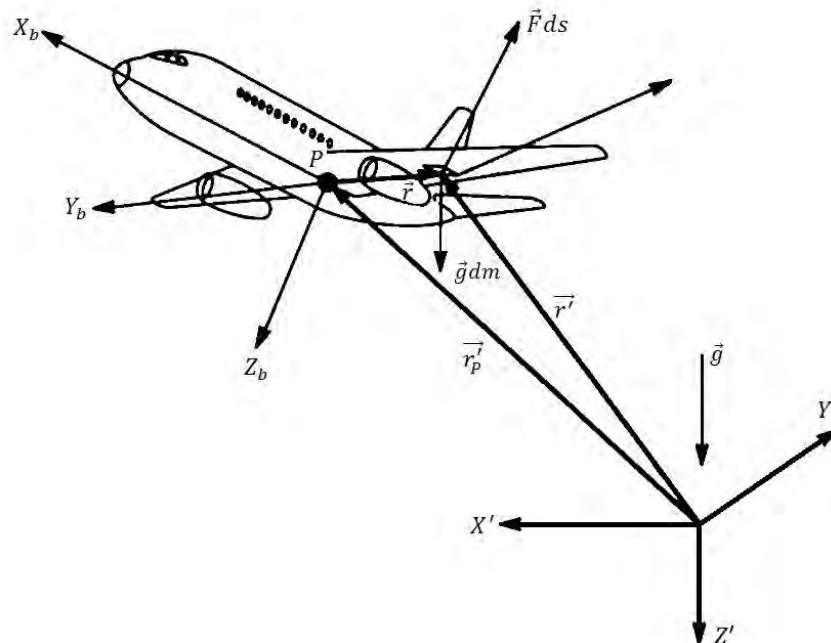


Figure 3.1: Body-fixed ($X_b Y_b Z_b$) and Earth-fixed ($X' Y' Z'$) coordinate system; Arrows indicate positive directions [40]

The airplane in Figure 3.1 is assumed rigid (except rotating machinery), consist of a continuum of mass elements, dm and these mass elements are kept track of by the vectors \vec{r}

and \vec{r}' , to the body and earth fixed reference frame, respectively. The vector \vec{r}'_P tracks of the origin of the body fixed frame i.e. center of gravity (CG) of the airplane (P), from the earth fixed frame. Each mass element is subject to the acceleration of gravity \vec{g} . Hence a force $\rho_A \vec{g} dv = \vec{g} dm$ acts on each one, where ρ_A represents the local mass density of the airplane. The mass elements located at the surface of the airplane are also subjected to a combined aerodynamic and thrust force per unit area \vec{F} . The forces $\rho_A \vec{g} dv$ and $\vec{F} ds$ are assumed to be the only external forces acting on the airplane.

3.3 Derivation of the Equations of Motion

According to Newton's Second Law, the time derivatives of linear and angular momenta of this airplane are equal to the externally applied forces and moments respectively [40]. In the vector integral form

$$\frac{d}{dt} \int_v \rho_A \frac{d\vec{r}'}{dt} dv = \int_v \rho_A \vec{g} dv + \int_s \vec{F} ds \quad (3.1)$$

$$\frac{d}{dt} \int_v \vec{r}' \times \rho_A \frac{d\vec{r}'}{dt} dv = \int_v \vec{r}' \times \rho_A \vec{g} dv + \int_s \vec{r}' \times \vec{F} ds \quad (3.2)$$

The integrals \int_v and \int_s represent volume and surface integrals for the entire airplane. These integrals can be evaluated only if the external geometry of the airplane is known. The total mass of the airplane is found from

$$m = \int_v \rho_A dv \quad (3.3)$$

There are two assumptions in this regard. One, total mass of the airplane remains constant with time

$$\frac{dm}{dt} = 0 \quad (3.4)$$

This assumption is justified as long as the mass change (due to fuel burning) is sufficiently small. Another, the mass distribution of the airplane is constant with time i.e.

Center of Gravity (CG) stays within a narrow range [40]. Now, to establish the relation between the position vectors, it can be denoted that

$$\vec{r}' = \vec{r}'_p + \vec{r} \quad (3.5)$$

As P is the center of gravity, the following relation must be satisfied

$$\int_v \vec{r} \rho_A dv = 0 \quad (3.6)$$

Now, putting Equations (3.5) and (3.6) in the left side of Equation (3.1), it is found that [40]

$$\frac{d}{dt} \int_v \rho_A \frac{d\vec{r}'}{dt} dv = m \frac{d}{dt} \frac{d\vec{r}'_p}{dt} = m \frac{d\vec{V}_P}{dt} \quad (3.7)$$

Where $\vec{V}_P = \frac{d\vec{r}'_p}{dt}$ is defined as the velocity of the airplane center of gravity.

For right side of Equation (3.1), assuming uniform gravitational field, the external forces are equal to the sum of gravitational force ($m\vec{g}$), total aerodynamic force (\vec{F}_A) and total thrust force (\vec{F}_T) [40]. Therefore

$$m \frac{d\vec{V}_P}{dt} = m\vec{g} + \vec{F}_A + \vec{F}_T \quad (3.8)$$

Next, the angular momentum Equation (3.2) needs to be further developed. Substitution of Equation (3.5) into Equation (3.2) while accounting for Equation (3.6) and (3.1) leads to [40]:

$$\frac{d}{dt} \int_v \vec{r} \times \frac{d\vec{r}'}{dt} \rho_A dv = \int_s \vec{r} \times \vec{F} ds = \vec{M}_A + \vec{M}_T \quad (3.9)$$

Where \vec{M}_A represents the total aerodynamic moment and \vec{M}_T represents the total thrust moment.

The volume integral is a time dependent function and this dependency can be eliminated by rewriting Equation (3.8) and (3.9) with respect to XYZ frame instead of $X'Y'Z'$. A problem is that coordinate system $X_bY_bZ_b$ is a rotating (non-inertial) coordinate system. In such a system Newton's Laws do not apply. However, by employing the following vector transformation relationship Newton's Laws can still be used.

$$\left. \frac{d\vec{A}}{dt} \right|_{fixed\ frame} = \left. \frac{\partial \vec{A}}{\partial t} \right|_{rotating\ frame} + \vec{\omega} \times \vec{A} \Big|_{coriolis\ component} \quad (3.10)$$

The vector \vec{A} represents any vector which is to be transformed. The vector $\vec{\omega}$ in Equation (3.10) is the angular rotation vector of system $X_b Y_b Z_b$ relative to system $X' Y' Z'$. The vector is also referred to as the angular velocity of the airplane relative to the earth. The latter is realistic because system $X_b Y_b Z_b$ was assumed to be body-fixed i.e. rigidly attached to the airplane and therefore moving with that. Applying this to Equation (3.8):

$$m \frac{d\vec{V}_P}{dt} = m \left(\dot{\vec{V}}_P + \vec{\omega} \times \vec{V}_P \right) = m\vec{g} + \vec{F}_A + \vec{F}_T \quad (3.11)$$

Now, for Equation (3.9), using vector cross product laws and conforming airplane as a rigid body with no spinning rotor i.e. $\vec{r} = \dot{\vec{r}} = 0$ in the left most side, it can be shown that

$$\int_v \vec{r} \times \left(\vec{\omega} \times \vec{r} + \vec{\omega} \times (\vec{\omega} \times \vec{r}) \right) \rho_A dv = \vec{M}_A + \vec{M}_T \quad (3.12)$$

It is obvious that $\vec{\omega}$ represents the angular acceleration of the airplane which is a property of body fixed frame. For that reason it can be taken outside of the integral, which makes the volume integral time independent.

Equations (3.11) and (3.12) are so called vector forms of the airplane equation of motion. To develop the scalar equivalents, these vectors are to be defined in axis level components with conventional unit vectors, depicted in Figure 3.2.

$$\vec{V}_p = iU + jV + kW \quad (3.13a)$$

$$\vec{r} = ix + jy + kz \quad (3.13b)$$

$$\vec{F}_A = iF_{Ax} + jF_{Ay} + kF_{Az} \quad (3.13c)$$

$$\vec{F}_T = iF_{Tx} + jF_{Ty} + kF_{Tz} \quad (3.13d)$$

$$\vec{g} = ig_x + jg_y + kg_z \quad (3.13e)$$

$$\vec{M}_A = iL_A + jM_A + kN_A \quad (3.13f)$$

$$\vec{M}_T = iL_T + jM_T + kN_T \quad (3.13g)$$

$$\vec{\omega} = iP + jQ + kR \quad (3.13h)$$

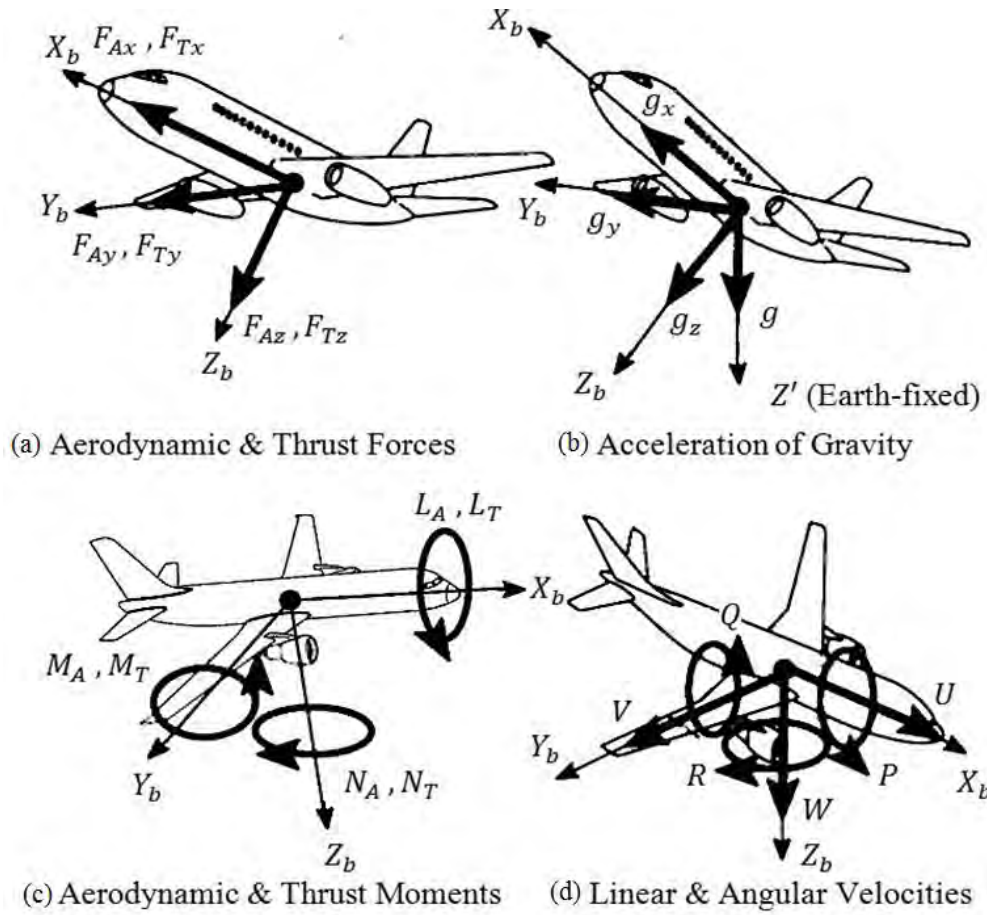


Figure 3.2: Definition of vector components in the airplane equations of motion [40];

(a) Forces (b) Gravity (c) Moments (d) Velocities

Thus, placing scalar components and equalizing both sides of Equation (3.11):

$$m(\dot{U} - VR + WQ) = mg_x + F_{Ax} + F_{Tx} \quad (3.14a)$$

$$m(\dot{V} - WP + UR) = mg_y + F_{Ay} + F_{Ty} \quad (3.14b)$$

$$m(\dot{W} - UQ + VP) = mg_z + F_{Az} + F_{Tz} \quad (3.14c)$$

Now, similarly, for Equation (3.12), after some steps of extensive vector manipulation, the moment equation comes into the following scalar form.

$$I_{xx}\dot{P} - I_{zx}\dot{R} - I_{zx}PQ + (I_{zz} - I_{yy})RQ = L_A + L_T \quad (3.15a)$$

$$I_{yy}\dot{Q} + (I_{xx} - I_{zz})PR + I_{zx}(P^2 - R^2) = M_A + M_T \quad (3.15b)$$

$$I_{zz}\dot{R} - I_{zx}\dot{P} + (I_{yy} - I_{xx})PQ + I_{zx}QR = N_A + N_T \quad (3.15c)$$

Where “ I ” terms are the moment and product of inertias of the airplane and they are defined in Equation (3.16).

$$\begin{aligned}
I_{xx} &= \int_v (y^2 + z^2) \rho_A dv \\
I_{yy} &= \int_v (z^2 + x^2) \rho_A dv \\
I_{zz} &= \int_v (x^2 + y^2) \rho_A dv \\
I_{xy} &= \int_v xy \rho_A dv = 0 \\
I_{yz} &= \int_v yz \rho_A dv = 0 \\
I_{zx} &= \int_v zx \rho_A dv
\end{aligned} \tag{3.16}$$

Notice that I_{xy} and I_{yz} are placed zeros as it is recognized that most airplanes are symmetrical about the ZX plane [40].

3.4 Axis Transformation

Equations (3.14) and (3.15) form six differential equation of motion with U, V, W, P, Q, R as dependent variables. Time is the independent variable. At this point it is not yet possible to solve these equations for the time histories of motion $U(t)$ through $R(t)$. Moreover, the gravity force components in Equation (3.14) depend on the orientation of the airplane relative to the earth-fixed coordinate system $X'Y'Z'$. To eliminate this, the inertial axis system has to be translated to the body axis system until its origin coincides with the center of gravity of the airplane and axes become parallel.

For this purpose, an intermediate reference frame $X_1Y_1Z_1$ is obtained that is parallel to the inertial frame. Now, the relative orientation of axis system $X_bY_bZ_b$ to axis system $X_1Y_1Z_1$ is defined with the help of three sequential rotations over the so-called Euler angles: the heading or azimuth angle (Ψ), the pitch angle (Θ), and the roll or bank angle (Φ).

- Rotation 1: $X_1Y_1Z_1$ is rotated about its Z_1 axis over an angle Ψ , then re-labeled as $X_2Y_2Z_2$.
- Rotation 2: $X_2Y_2Z_2$ is rotated about its Y_2 axis over an angle Θ , then re-labeled as $X_3Y_3Z_3$.
- Rotation 3: $X_3Y_3Z_3$ is rotated about X_3 axis over an angle Φ , so it coincides with $X_bY_bZ_b$.

It is difficult to visualize the actual sequence of rotations in a single drawing, as shown in Figure 3.3, so the sequence is illustrated with three separate drawings in Figure 3.4.

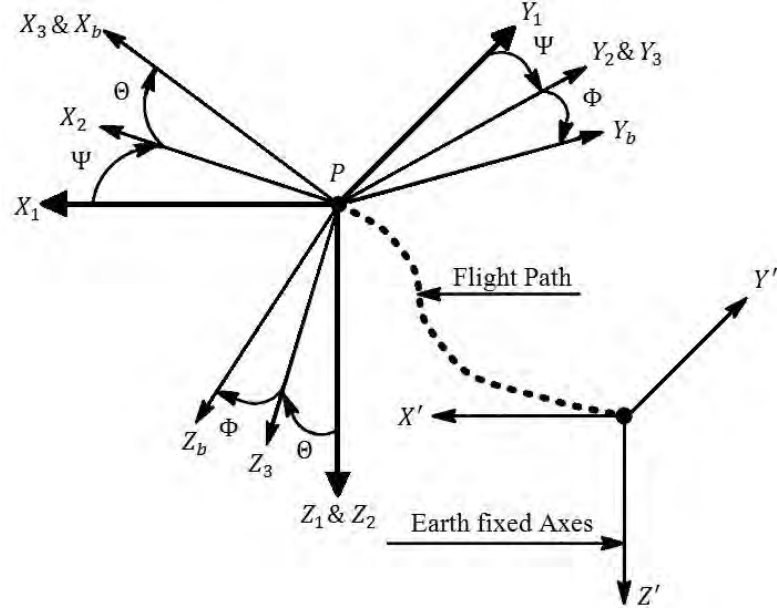


Figure 3.3: Airplane Orientation with Euler Angles [40]

With the help of the rotation matrix defined by this Euler angles, the components of the velocity vector \vec{V}_P can be represented as

$$\begin{bmatrix} U' \\ V' \\ W' \end{bmatrix} = \begin{bmatrix} \dot{x}' \\ \dot{y}' \\ \dot{z}' \end{bmatrix} = \begin{bmatrix} \cos\Psi & -\sin\Psi & 0 \\ \sin\Psi & \cos\Psi & 0 \\ 0 & 0 & 1 \end{bmatrix} \begin{bmatrix} \cos\Theta & 0 & \sin\Theta \\ 0 & 1 & 0 \\ -\sin\Theta & 0 & \cos\Theta \end{bmatrix} \begin{bmatrix} 1 & 0 & 0 \\ 0 & \cos\Phi & -\sin\Phi \\ 0 & \sin\Phi & \cos\Phi \end{bmatrix} \begin{bmatrix} U \\ V \\ W \end{bmatrix} \quad (3.17)$$

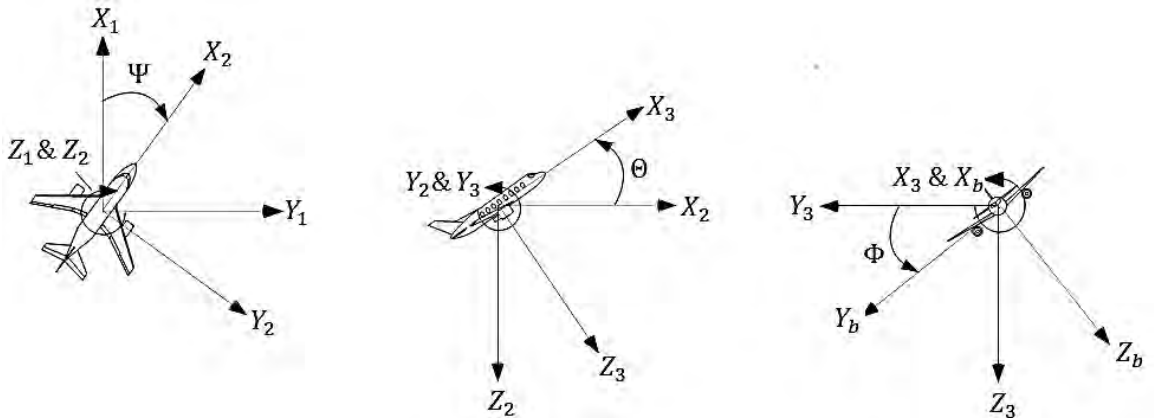


Figure 3.4: Illustration of Figure 3.3, rotation sequence from left to right

This equation provides the desired relationship between velocity components in the earth-fixed system $X'Y'Z'$ and those in the body-fixed system $X_bY_bZ_b$. So the flight path of the airplane in terms of $x'(t)$, $y'(t)$ and $z'(t)$ can be found by integrating it. To do that, the

Euler angles Ψ , Θ and Φ must be known. By definition

$$\vec{\omega} = iP + jQ + kR = \vec{\dot{\Psi}} + \vec{\dot{\Theta}} + \vec{\dot{\Phi}} \quad (3.18)$$

Using the equality of this equation and the same coordinate transformation rules that is used earlier, it can be proved that

$$P = \dot{\Phi} - \dot{\Psi} \sin\Theta \quad (3.19a)$$

$$Q = \dot{\Theta} \cos\Phi + \dot{\Psi} \cos\Theta \sin\Phi \quad (3.19b)$$

$$R = \dot{\Psi} \cos\Theta \cos\Phi - \dot{\Theta} \sin\Phi \quad (3.19c)$$

These are known as the Kinematics equations of an airplane [40]. For the flight path integration problem, it is desirable to invert these equations to yield:

$$\dot{\Psi} = (Q \sin\Phi + R \cos\Phi) \sec\Theta \quad (3.20a)$$

$$\dot{\Theta} = Q \cos\Phi - R \sin\Phi \quad (3.20b)$$

$$\dot{\Phi} = P + Q \sin\Phi \tan\Theta + R \cos\Phi \tan\Theta \quad (3.20c)$$

Another thing that is to take into account is the contribution of gravity force in the force equations i.e. Equation (3.14). Through the process of axes transformation, assuming flat earth, it can be easily understood at this moment that

$$g_x = -g \sin\Theta \quad (3.21a)$$

$$g_y = g \sin\Phi \cos\Theta \quad (3.21b)$$

$$g_z = g \cos\Phi \cos\Theta \quad (3.21c)$$

So the modified force equations are

$$m(\dot{U} - VR + WQ) = -mg \sin\Theta + F_{Ax} + F_{Tx} \quad (3.22a)$$

$$m(\dot{V} - WP + UR) = mg \sin\Phi \cos\Theta + F_{Ay} + F_{Ty} \quad (3.22b)$$

$$m(\dot{W} - UQ + VP) = mg \cos\Phi \cos\Theta + F_{Az} + F_{Tz} \quad (3.22c)$$

Equations (3.22) and (3.16) represent the inertial forces and moments acting on the airplane. All the forces are proportional to the mass of the airplane. Consequently, these terms may be conveniently combined into components to represent the accelerations which would be measured by sensors located on the airplane in such a manner that the input axes of the sensors would be coincident with the body axes. For convenience, the force and moments

are renamed in accordance to the axis components in this manner.

$$F_{Ax} + F_{Tx} = X \quad (3.23a)$$

$$F_{Ay} + F_{Ty} = Y \quad (3.23b)$$

$$F_{Az} + F_{Tz} = Z \quad (3.23c)$$

$$L_A + L_T = L \quad (3.23d)$$

$$M_A + M_T = M \quad (3.23e)$$

$$N_A + N_T = N \quad (3.23f)$$

Putting Equation (3.23) into Equation (3.22), the force equations of the airplane for the body fixed axis system are

$$X = m(\dot{U} - VR + WQ + g \sin\Theta) \quad (3.24a)$$

$$Y = m(\dot{V} - WP + UR - g \sin\Phi \cos\Theta) \quad (3.24b)$$

$$Z = m(\dot{W} - UQ + VP - g \cos\Phi \cos\Theta) \quad (3.24c)$$

For convenience, the moment equations of the airplane for the body fixed axis system that is derived in Equation (3.15), is presented below.

$$L = I_{xx} \dot{P} - I_{zx} \dot{R} - I_{zx} PQ + (I_{zz} - I_{yy}) QR \quad (3.25a)$$

$$M = I_{yy} \dot{Q} + (I_{xx} - I_{zz}) PR + I_{zx} (P^2 - R^2) \quad (3.25b)$$

$$N = I_{zz} \dot{R} - I_{zx} \dot{P} + (I_{yy} - I_{xx}) PQ + I_{zx} QR \quad (3.25c)$$

And finally, the kinematic equations of Equation (3.20):

$$\dot{\Psi} = (Q \sin\Phi + R \cos\Phi) \sec\Theta \quad (3.26a)$$

$$\dot{\Theta} = Q \cos\Phi - R \sin\Phi \quad (3.26b)$$

$$\dot{\Phi} = P + Q \sin\Phi \tan\Theta + R \cos\Phi \tan\Theta \quad (3.26c)$$

Equations (3.24) to (3.26) are referred to as the general airplane nonlinear equations of motion. It is rather generous description considering the assumptions that served to reduce the generality of these equations.

3.5 Angle of Attack, Sideslip Angle, Flight Path Angle

Before proceeding further, it is necessary to include the definitions of the angles associated with airplane path trajectory. A general idea of the angle of attack is placed in Chapter 2. As airplane body fixed coordinate system and the velocity parameters are vividly defined in the previous section, therefore, mathematically, angle of attack (α), sideslip angle (β) and flight path angle (γ) can be defined as [43]:

$$\alpha = \tan^{-1} \frac{W}{U} \quad (3.27a)$$

$$\beta = \sin^{-1} \frac{V}{|\vec{V}_P|} \quad (3.27b)$$

$$\gamma = \Theta - \alpha \quad (3.27c)$$

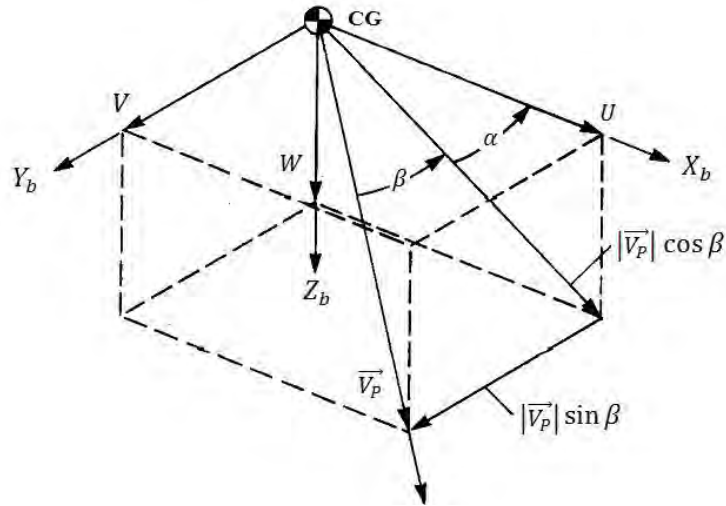


Figure 3.5: Angle of attack (α) and sideslip angle (β) [43]

Where $|\vec{V}_P|$ is the velocity of the airplane center of gravity, as defined early in this chapter.

From Figure 3.5, other velocity parameters can be identified as

$$U = |\vec{V}_P| \cos \alpha \cos \beta \quad (3.28a)$$

$$V = |\vec{V}_P| \sin \beta \quad (3.28b)$$

$$W = |\vec{V}_P| \sin \alpha \cos \beta \quad (3.28c)$$

$$|\vec{V}_P| = \sqrt{U^2 + V^2 + W^2} \quad (3.28d)$$

Now, the flight path angle and angle of attack are more understandable from the side view as shown in Figure 3.6. It is obvious that in level flight $\Theta = \alpha$.

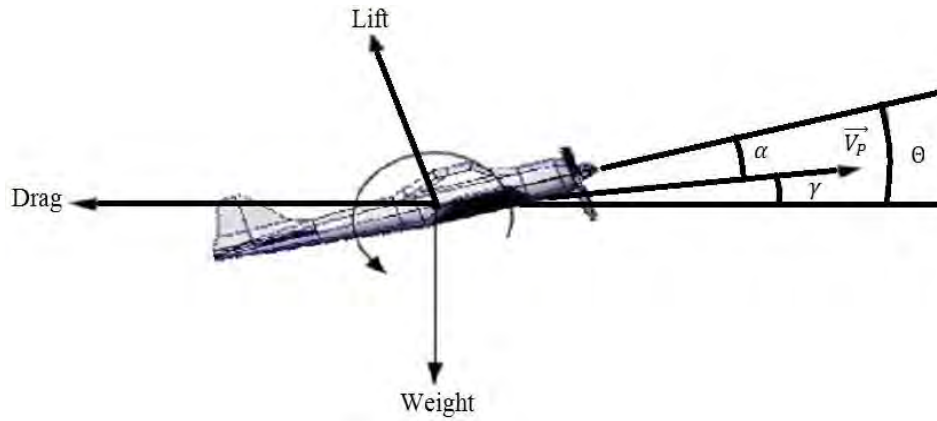


Figure 3.6: Angle of attack (α), sideslip angle (β), pitch angle (Θ) [43]

3.6 Stability and Wind Reference Frames

These two axis system are often used in flight dynamics as because in certain cases, the use of these coordinate system reduce complexity of airplane equations of motion.

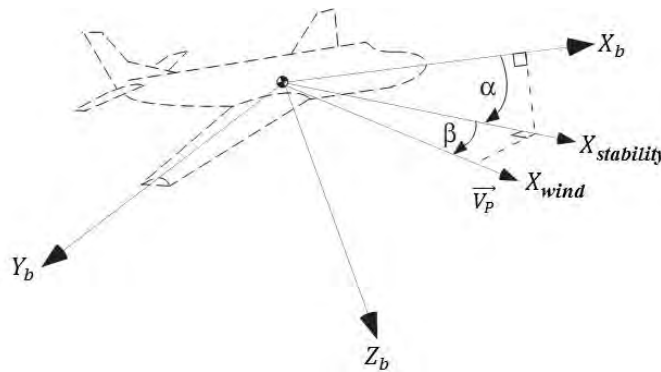


Figure 3.7: Stability and wind frame [43]

These stability and wind frames rather characterize the angle of attack (α), and the sideslip angle (β). As discussed, these aerodynamic angles are defined by means of coordinate rotations from the body frame. The first rotation, about the Y_b axis, defines the stability frame; and the angle is the angle of attack. With no sideslip, it is the deviation of the velocity vector \vec{V}_P , or the airplane flight path from the body fixed frame.

The second rotation leads to the wind frame, and the side-slip angle is the angle between the stability frame and the wind frame. An airplane has sideslip if its velocity vector is not in the $X_b Z_b$ plane, which might be due to gust, crosswind or any unwanted airflow, or

it could not make a coordinated turn.

Equations (3.28) to (3.30) show the direction cosine matrices (DCM) that define the transformations between the coordinated frames.

$$\begin{bmatrix} X_{ST} \\ Y_{ST} \\ Z_{ST} \end{bmatrix} = \begin{bmatrix} \cos \alpha & 0 & \sin \alpha \\ 0 & 1 & 0 \\ -\sin \alpha & 0 & \cos \alpha \end{bmatrix} \begin{bmatrix} X_b \\ Y_b \\ Z_b \end{bmatrix} \quad (3.29)$$

$$\begin{bmatrix} X_W \\ Y_W \\ Z_W \end{bmatrix} = \begin{bmatrix} \cos \beta & \sin \beta & 0 \\ -\sin \beta & \cos \beta & 0 \\ 0 & 0 & 1 \end{bmatrix} \begin{bmatrix} X_{ST} \\ Y_{ST} \\ Z_{ST} \end{bmatrix} \quad (3.30)$$

$$\begin{bmatrix} X_W \\ Y_W \\ Z_W \end{bmatrix} = \begin{bmatrix} \cos \beta \cos \alpha & \sin \beta & \cos \beta \sin \alpha \\ -\sin \beta \cos \alpha & \cos \beta & -\sin \beta \sin \alpha \\ -\sin \alpha & 0 & \cos \alpha \end{bmatrix} \begin{bmatrix} X_b \\ Y_b \\ Z_b \end{bmatrix} \quad (3.31)$$

3.7 Linearization of Equations of Motion

The equations of motion depicted in Equation (3.24) (3.25) and (3.26) are non-linear since they contain terms which comprise the product of dependent variables, the squares of dependent variables, and some of the terms are transcendental. Solutions of such equations cannot be obtained analytically and would require the use of computer. Some simplification is possible, however, by considering the airplane to comprise two components: a mean motion which represents the equilibrium, or trim conditions, and a dynamic motion which accounts for the perturbations about the mean motion [27]. In this form of analysis it is customary to assume that the perturbations are small. Thus, every motion variable is considered to have two components. For example:

$$\begin{aligned} U &= U_0 + u & V &= V_0 + v & W &= W_0 + w; \\ P &= P_0 + p & Q &= Q_0 + q & R &= R_0 + r; \\ \Psi &= \Psi_0 + \psi & \Theta &= \Theta_0 + \theta & \Phi &= \Phi + \phi; \\ X &= X_0 + x & Y &= Y_0 + y & Z &= Z_0 + z; \\ L &= L_0 + l & M &= M_0 + m_1 & N &= N_0 + n; & \dots \dots \text{etc} \end{aligned} \quad (3.32)$$

The trim, or equilibrium, values are denoted by a subscript 0 and the small perturbation values of a variable are denoted by the lower case letter. In trim there can be no translational

or rotational acceleration i.e. $\dot{U} = \dot{V} = \dot{W} = \dot{P} = \dot{Q} = \dot{R} = 0$. Hence, the equations which represent the trim conditions can be expressed as [43]:

$$X_0 = m(-V_0 R_0 + W_0 Q_0 + g \sin \Theta_0) \quad (3.33a)$$

$$Y_0 = m(-W_0 P_0 + U_0 R_0 - g \sin \Phi_0 \cos \Theta_0) \quad (3.33b)$$

$$Z_0 = m(-U_0 Q_0 + V_0 P_0 - g \cos \Phi_0 \cos \Theta_0) \quad (3.33c)$$

$$L_0 = -I_{zx} P_0 Q_0 + (I_{zz} - I_{yy}) Q_0 R_0 \quad (3.33d)$$

$$M_0 = (I_{xx} - I_{zz}) P_0 R_0 + I_{zx} (P_0^2 - R_0^2) \quad (3.33e)$$

$$N_0 = (I_{yy} - I_{xx}) P_0 Q_0 + I_{zx} Q_0 R_0 \quad (3.33f)$$

Steady rolling, pitching and yawing motion can occur in the trim condition; the equations which define P_0, Q_0 and R_0 are given by Equation (3.26) but with Ψ, Θ and Φ being subscripted by 0.

The perturbed motion can be found either by substituting Equation (3.32) into (3.24) and (3.25), expanding the terms and then subtracting Equation (3.33) from the result, or by differentiating both sides of Equations (3.24) and (3.25). When perturbations from the mean conditions are small, the sines and cosines can be approximated to the angles themselves and the value unity, respectively. Moreover, the products and squares of the perturbed quantities are negligible. Thus, the perturbed equations of motion for an airplane can be written as [43]:

$$dX = m[\dot{u} - V_0 r - v R_0 + W_0 q + w Q_0 + g \theta \cos \Theta_0] \quad (3.34a)$$

$$dY = m[\dot{v} - W_0 p - w P_0 + U_0 r + u R_0 - g(\phi \cos \Theta_0 \cos \Phi_0 - \theta \sin \Theta_0 \sin \Phi_0)] \quad (3.34b)$$

$$dZ = m[\dot{w} - U_0 q - u Q_0 + V_0 p + v P_0 + g(\phi \cos \Theta_0 \sin \Phi_0 + \theta \sin \Theta_0 \cos \Phi_0)] \quad (3.34c)$$

$$dL = I_{xx} \dot{p} - I_{zx} \dot{r} - I_{zx} (P_0 q + p Q_0) + (I_{zz} - I_{yy})(Q_0 r + q R_0) \quad (3.34d)$$

$$dM = I_{yy} \dot{q} + (I_{xx} - I_{zz})(P_0 r + p R_0) + I_{zx} (2P_0 p - 2R_0 r) \quad (3.34e)$$

$$dN = I_{zz} \dot{r} - I_{zx} \dot{p} + (I_{yy} - I_{xx})(P_0 q + Q_0 p) + I_{zx} (Q_0 r + R_0 q) \quad (3.34f)$$

Where Ψ_0, Θ_0 and Φ_0 have been used to represent steady orientations, and Ψ, Θ and Φ are the perturbations in the Euler angles. Equations (3.34) are now linear. Obviously, perturbation equations are required for the auxiliary set of equations given as Equation (3.19), because the gravitational forces must be perturbed by any small change in the orientation of the body axis system with respect to the Earth axis system. However, the full

set of perturbed, auxiliary equations is rarely used since it is complicated. But the components of angular velocity which represent the rotation of the body-fixed axes relative to the Earth axes are sometimes required. These are:

$$p = \dot{\phi} - \dot{\Psi}_0 \theta \cos\theta_0 - \dot{\psi} \sin\theta_0 \quad (3.35a)$$

$$q = \dot{\theta} \cos\Phi_0 - \dot{\Theta}_0 \phi \sin\Phi_0 + \dot{\Psi}_0 \phi \cos\theta_0 \cos\Phi_0 - \dot{\Psi}_0 \theta \sin\theta_0 \sin\Phi_0 + \dot{\psi} \cos\theta_0 \sin\Phi_0 \quad (3.35b)$$

$$r = \dot{\psi} \cos\theta_0 \cos\Phi_0 - \dot{\Psi}_0 \phi \cos\theta_0 \sin\Phi_0 - \dot{\Psi}_0 \theta \sin\theta_0 \cos\Phi_0 - \dot{\Theta}_0 \phi \cos\Phi_0 - \dot{\theta} \sin\Phi_0 \quad (3.35c)$$

The combined Equations (3.34) and (3.35) are the nine perturbed equations of motion relative to a very general steady state: i.e. one for which all motion variables are allowed to have non-zero steady state values [43]. It turns out that the majority of airplane dynamic stability problems are concerned with perturbed motions relative to a wings level, steady state, straight line flight condition with a relatively small flight path angle. For such a steady state the following conditions hold:

- a. No initial steady state side velocity exists: $V_0 = 0$
- b. No initial bank angle exists: $\Phi_0 = 0$
- c. No initial angular velocities exist: $P_0 = Q_0 = R_0 = \dot{\Psi}_0 = \dot{\Theta}_0 = \dot{\Phi}_0 = 0$

When these special steady state conditions are introduced into Equations (3.34) and (3.35), the equations become

$$dX = m(\dot{u} - W_0 q + g \theta \cos\theta_0) \quad (3.36a)$$

$$dY = m(\dot{v} - W_0 p + U_0 r - g \phi \cos\theta_0) \quad (3.36b)$$

$$dZ = m(\dot{w} - U_0 q + g \theta \sin\theta_0) \quad (3.36c)$$

$$dL = I_{xx} \dot{p} - I_{zx} \dot{r} \quad (3.37a)$$

$$dM = I_{yy} \dot{q} \quad (3.37b)$$

$$dN = I_{zz} \dot{r} - I_{zx} \dot{p} \quad (3.37c)$$

$$p = \dot{\phi} - \dot{\psi} \sin\theta_0 \quad (3.38a)$$

$$q = \dot{\theta} \quad (3.38b)$$

$$r = \dot{\psi} \cos\theta_0 \quad (3.38c)$$

These equations are the basis for the dynamic stability analysis of airplane.

Consideration of Equations (3.37) and (3.38) indicates not only that the equations have been simplified, but that the set can be separated into two distinct groups which are given below:

$$dX = m(\dot{u} - W_0 q + g \theta \cos\Theta_0) \quad (3.39a)$$

$$dZ = m(\dot{w} - U_0 q + g \theta \sin\Theta_0) \quad (3.39b)$$

$$dM = I_{yy} \dot{q} \quad (3.39c)$$

$$dY = m(\dot{v} - W_0 p + U_0 r - g \phi \cos\Theta_0) \quad (3.40a)$$

$$dL = I_{xx} \dot{p} - I_{zx} \dot{r} \quad (3.40b)$$

$$dN = I_{zz} \dot{r} - I_{zx} \dot{p} \quad (3.40c)$$

To expand the left-hand side of the equations of motion, a Taylor series is used about the trimmed flight condition. Thus, for example,

$$dZ = \frac{\partial Z}{\partial u} u + \frac{\partial Z}{\partial \dot{u}} \dot{u} + \frac{\partial Z}{\partial w} w + \frac{\partial Z}{\partial \dot{w}} \dot{w} + \frac{\partial Z}{\partial q} q + \frac{\partial Z}{\partial \dot{q}} \dot{q} + \frac{\partial Z}{\partial \delta_E} \delta_E + \frac{\partial Z}{\partial \dot{\delta}_E} \dot{\delta}_E \quad (3.41)$$

Equation (3.41) supposes that the perturbed force dZ has a contribution from only one control surface, the elevator and hence the elevator deflection angle δ_E is inserted. However, if any other control surface on the airplane being considered were involved, additional terms, accounting for their contribution to dZ , would be used. This is generally known as component build up process. For example, if changes of thrust (T), and the deflection of flaps (F) and symmetrical spoilers (sp) were also used as controls for longitudinal motion, additional terms, such as

$$\frac{\partial Z}{\partial \delta_T} \delta_T, \frac{\partial Z}{\partial \delta_F} \delta_F \text{ and } \frac{\partial Z}{\partial \delta_{sp}} \delta_{sp}$$

would be added to Equation (3.41). Furthermore, some terms depending on other motion variables, such as θ , are omitted because they are generally insignificant.

Suppose, for the moment only longitudinal motion is treated, and, for simplicity, it is assumed that only elevator deflection is involved in the control of the airplane's longitudinal motion. Thus, it is now possible to write Equation (3.39) as:

$$\frac{\partial X}{\partial u}u + \frac{\partial X}{\partial \dot{u}}\dot{u} + \frac{\partial X}{\partial w}w + \frac{\partial X}{\partial \dot{w}}\dot{w} + \frac{\partial X}{\partial q}q + \frac{\partial X}{\partial \dot{q}}\dot{q} + \frac{\partial X}{\partial \delta_E}\delta_E + \frac{\partial X}{\partial \dot{\delta}_E}\dot{\delta}_E \quad (3.42a)$$

$$= m(\dot{u} - W_0q + g \theta \cos\Theta_0)$$

$$\frac{\partial Z}{\partial u}u + \frac{\partial Z}{\partial \dot{u}}\dot{u} + \frac{\partial Z}{\partial w}w + \frac{\partial Z}{\partial \dot{w}}\dot{w} + \frac{\partial Z}{\partial q}q + \frac{\partial Z}{\partial \dot{q}}\dot{q} + \frac{\partial Z}{\partial \delta_E}\delta_E + \frac{\partial Z}{\partial \dot{\delta}_E}\dot{\delta}_E \quad (3.42b)$$

$$= m(\dot{w} - U_0q + g \theta \sin\Theta_0)$$

$$\frac{\partial M}{\partial u}u + \frac{\partial M}{\partial \dot{u}}\dot{u} + \frac{\partial M}{\partial w}w + \frac{\partial M}{\partial \dot{w}}\dot{w} + \frac{\partial M}{\partial q}q + \frac{\partial M}{\partial \dot{q}}\dot{q} + \frac{\partial M}{\partial \delta_E}\delta_E + \frac{\partial M}{\partial \dot{\delta}_E}\dot{\delta}_E = I_{yy}\dot{q} \quad (3.42c)$$

To simplify the notation it is customary to make the following substitutions:

$$X_x = \frac{1}{m} \frac{\partial X}{\partial x} \quad (3.43a)$$

$$Z_x = \frac{1}{m} \frac{\partial Z}{\partial x} \quad (3.43b)$$

$$M_x = \frac{1}{I_{yy}} \frac{\partial M}{\partial x} \dots \dots etc \quad (3.43c)$$

When this substitution is made, the coefficients, such as X_x , Z_x , and M_x etc. are combination of terms referred to as the stability and control derivatives. For example, X_x signifies the acceleration of the airplane along the X_b axis due to the change in velocity u .

3.8 Equations of Longitudinal Motion

Finally, using notations of Equation (3.43), Equation (3.42) can be written as

$$\begin{aligned} \dot{u} = & X_u u + X_{\dot{u}} \dot{u} + X_w w + X_{\dot{w}} \dot{w} + X_q q + X_{\dot{q}} \dot{q} - W_0 q \\ & - g \cos\Theta_0 \theta + X_{\delta_E} \delta_E + X_{\dot{\delta}_E} \dot{\delta}_E \end{aligned} \quad (3.44a)$$

$$\begin{aligned} \dot{w} = & Z_u u + Z_{\dot{u}} \dot{u} + Z_w w + Z_{\dot{w}} \dot{w} + Z_q q + Z_{\dot{q}} \dot{q} + U_0 q \\ & - g \sin\Theta_0 \theta + Z_{\delta_E} \delta_E + Z_{\dot{\delta}_E} \dot{\delta}_E \end{aligned} \quad (3.44b)$$

$$\dot{q} = M_u u + M_{\dot{u}} \dot{u} + M_w w + M_{\dot{w}} \dot{w} + M_q q + M_{\dot{q}} \dot{q} + M_{\delta_E} \delta_E + M_{\dot{\delta}_E} \dot{\delta}_E \quad (3.44c)$$

$$\dot{\theta} = q \quad (3.44d)$$

From studying the aerodynamic data of a large number of airplanes, it is evident that not every stability derivative is significant and, frequently, a number can be neglected [43]. However, it is essential to remember that such stability derivatives depend both upon the airplane being considered and the flight condition which applies. Thus, before ignoring

stability derivatives, it is important to check the appropriate aerodynamic data. Without loss of generality it can be assumed that the following stability derivatives are often insignificant, and may be ignored:

$$X_{\dot{u}}, X_q, X_{\dot{w}}, X_{\delta_E}, Z_{\dot{u}}, Z_{\dot{w}}, M_{\dot{u}}, Z_{\delta_E} \text{ and } M_{\delta_E}$$

With these assumptions, the final equations of perturbed longitudinal motion, for straight, symmetric flight, with wings level, can be expressed as:

$$\dot{u} = X_u u + X_w w - W_0 q - g \cos \Theta_0 \theta \quad (3.45a)$$

$$\dot{w} = Z_u u + Z_w w + U_0 q - g \sin \Theta_0 \theta + Z_{\delta_E} \delta_E \quad (3.45b)$$

$$\dot{q} = M_u u + M_w w + M_{\dot{w}} \dot{w} + M_q q + M_{\delta_E} \delta_E \quad (3.45c)$$

$$\dot{\theta} = q \quad (3.45d)$$

Using the stability axis system, in which $W_0 = 0$ and $\Theta_0 = \gamma_0$, as shown before, Equation (3.45) may be expressed as

$$\dot{u} = X_u u + X_w w - g \cos \gamma_0 \theta \quad (3.46a)$$

$$\dot{w} = Z_u u + Z_w w + U_0 q - g \sin \gamma_0 \theta + Z_{\delta_E} \delta_E \quad (3.46b)$$

$$\dot{q} = M_u u + M_w w + M_{\dot{w}} \dot{w} + M_q q + M_{\delta_E} \delta_E \quad (3.46c)$$

$$\dot{\theta} = q \quad (3.46d)$$

3.9 Stability and Control Derivatives for Longitudinal Motion

In order to solve Equation (3.45), the values of all the coefficients have to be known. $X_u, X_w, Z_u, Z_w, M_u, M_w, M_{\dot{w}}, M_q$ are the stability derivatives and $Z_{\delta_E}, M_{\delta_E}$ are the control derivatives [43].

The stability derivative X_u can be expressed as

$$X_u = \frac{1}{m} \frac{\partial X}{\partial u} = \frac{1}{m} \frac{\partial}{\partial u} \left(\frac{1}{2} \rho u^2 S C_X \right) = \frac{\rho S U_0}{m} [2C_{X_0} + C_{X_u}] \quad (3.47)$$

Where

$$C_{X_u} = \frac{\partial C_X}{\partial (u/u_0)} \quad (3.48)$$

C_{X_u} is the derivative of the dimensionless X -force coefficient with respect to the dimensionless velocity u/u_0 . Note that the first term in the final expression of Equation (3.47) arises because the dynamic pressure, which is a function of the flight velocity $u_0 + u$. Similar expressions can be developed for all the required derivatives as shown below [43].

$$Z_w = \frac{\rho S U_0}{2m} (C_{L_\alpha} + C_{D_\alpha}) \quad (3.49)$$

$$M_u = \frac{\rho S U_0 \bar{c}}{I_{yy}} (C_{m_u} + C_{m_\alpha}) \quad (3.50)$$

$$M_w = \frac{\rho S U_0 \bar{c}}{2I_{yy}} C_{m_\alpha} \quad (3.51)$$

$$M_{\dot{w}} = \frac{\rho S \bar{c}^2}{4I_{yy}} C_{m_{\dot{\alpha}}} \quad (3.52)$$

$$M_q = \frac{\rho S U_0 \bar{c}^2}{4I_{yy}} C_{m_q} \quad (3.53)$$

$$M_{\delta_E} = \frac{\rho U_0^2 S \bar{c}}{2I_{yy}} C_{m_{\delta_E}} \quad (3.54)$$

$$Z_{\delta_E} = -\frac{\rho U_0^2 S}{2m} C_{L_{\delta_E}} \quad (3.55)$$

Where

C_{L_α} = Lift Coefficient due to Basic Geometry

C_{D_α} = Drag Coefficient due to Basic Geometry

C_{m_u} = Pitching Moment Coefficient due to Forward Speed

C_{m_α} = Pitching Moment Coefficient due to Basic Geometry

$C_{m_{\dot{\alpha}}}$ = Pitching Moment Coefficient due to Change in AOA

C_{m_q} = Pitching Moment Coefficient due to Pitch Rate

$C_{m_{\delta_E}}$ = Pitching Moment Coefficient due to Elevator Deflection

$C_{L_{\delta_E}}$ = Lift Coefficient due to Elevator Deflection

CHAPTER 4

THE MODEL UAV – ENA-01

4.1 Introduction

UAVs can be remote controlled or fly autonomously based on pre-programmed flight plans. They are currently used in a number of military roles, including reconnaissance and attack. They are also used in civil applications such as firefighting where a human observer would be at risk, police observation of civil disturbances and scenes of crimes, and patrol support in time of natural disasters. There is a wide variety UAV shape, size, configuration and characteristic as they are built depending upon the purpose intended to serve. In recent years, there has been enormous research and development in this area and lots of them are commercially available.



Figure 4.1: ENA-01

4.2 ENA-01 Specifications

The UAV that is used in this research (ENA-01) is a remote controlled UAV, serving as a prototype of a short range civil aircraft. The intended work was to implant a controller in it so that it could be semi-autonomous in the pitch plane and therefore eliminate any disturbance that may come in the way of executing an elevator command. Therefore a

controller for the ENA-01 airframe is designed and simulated in MATLAB Simulink environment.

ENA-01 has ailerons, elevator and rudder as flight control surfaces for maneuvering purpose, even though the research concern is limited to pitch command stabilization. A detail description of the ENA-01 is given in Table 4.1.

Table 4.1: Technical Specifications of ENA-01

Identity		Description
Weight		1.5kg
Structure Material		Aluminum Bar, Cork-sheet, Hardboard
Fuselage length		1.0 m
Wing	Wing Type	Straight with Winglet
	Wingspan	1.52 m
	Wing Surface Area	0.32 m ²
	Wing Mean Aerodynamic Chord	0.21 m
Propulsion	Propulsion System	Single Wooden Propeller at nose
	Propeller Diameter	0.16m
	Propeller Blade Angle	2 degree
	Propeller Thrust	1.2 kg
Power Plant		380 watt Brushless DC motor
Electrical Power		11.1V Battery
Range		2 km
Takeoff Speed		30km/h
Takeoff Field length		40 m (can be hand launched)
Endurance		30 minutes
Maximum Cruise Speed		60 km/h
Control Surfaces		Ailerons (2), Elevator (1), Rudder (1)
Control Surface Actuators		DC Servo Motors (4)

CHAPTER 5

THE DESIGN PROCESS

5.1 Introduction

As stated earlier, to construct a flight dynamics model for ENA-01, the software Datcom+ Pro is used in this research to simulate the airframe and calculate the aerodynamic coefficients. By writing an input file containing all essential geometries of an airplane, Datcom produces an output file with stability derivatives according to the specified flight conditions. The interface to Simulink is achieved by ‘Digital DATCOM Forces and Moments’ block in the Aerospace Blockset of Simulink. Therefore, interlinking Datcom with Simulink in the frontend, an airplane model for any fixed wing UAVs can be rapidly developed without wind tunnel testing or Computational Fluid Dynamics (CFD) analysis. This feature significantly increases the repeatability of flight simulation and is found very useful for UAV preliminary control designs, where only a rough estimate of the vehicle’s stability is required. Data visualization is another aspect considered which has led to interfacing the flight dynamics model with an open source flight simulation program FlightGear that can produce a 3D graphic animation in real time. The animation facility allows the UAV to be viewed from any angle, and provides absolute visual information on the UAV attitude and stability. With the FlightGear added in the back-end, the complete simulation environment is shown in Figure 5.1.

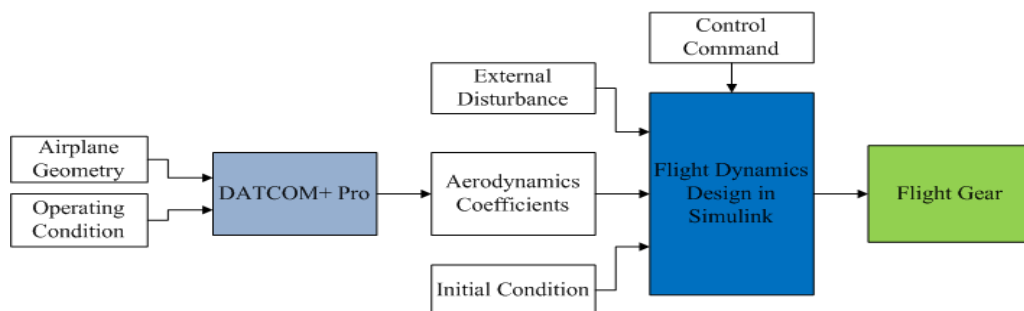


Figure 5.1: Block diagram of integrated flight dynamics modeling

5.2 ENA-01 Modeling by Datcom+ Pro

The Digital Datcom program uses aircraft-unique configuration and geometry parameters to predict aircraft performance by utilizing classical aerodynamic equations. It calculates static stability, high lift and control, and dynamic derivative characteristics, and is applicable to subsonic, transonic, supersonic, and hypersonic vehicles, for traditional body-wing-tail or canard-equipped vehicles. Coefficient data output by Datcom is presented as a function of angle of attack at up to 20 user-defined values of angle of attack, and up to 9 user-defined values of surface deflection for flaps, ailerons and elevator.

For those speed regimes and configurations where Datcom methods are available, the Digital Datcom output provides the longitudinal coefficients C_L , C_d , C_m , C_N , and C_A (body axis), and the derivatives $dC_L/d\alpha$, $dC_m/d\alpha$, $dC_Y/d\beta$, $dC_n/d\beta$, and $dC_l/d\beta$. Output for configurations with a wing and horizontal tail also includes downwash and the local dynamic pressure ratio in the region of the tail. The pitch, roll, yaw and angle-of-attack rate derivatives dC_L/dq , dC_m/dq , $dC_L/d\dot{\alpha}$, $dC_m/d\dot{\alpha}$, dC_l/dp , dC_Y/dp , dC_n/dp , dC_n/dr , and dC_l/dr are also computed for most configurations. The determination of these terms, and others which are not included here is covered extensively in standard airplane design textbooks. It has to be kept in mind that all these values are in stability axis system and Datcom provides predicted data only up to stall. Detail of these coefficients are discussed in Appendix I.

The front end of Datcom is a **.dcm** file that comprises a series of NAMELIST statements, listing input variables which describe the aircraft under consideration and variables which control the execution and output of Datcom. The source code editor used is *Notepad++*. The input file for ENA-01 with their remarks is placed in Appendix II.

Unless specified, execution of the **.dcm** file using Datcom+ Pro program generates the following output files

- **.out** – the original FOR006.DAT output file format, that includes the input data cards and all coordinated aerodynamic coefficients. This file can be imported into MATLAB for further analysis.
- **.xml** – a file format for input into JSBSim, an open-source Flight Dynamics model.
- **.csv** – Comma-separated values format which can be easily opened with Microsoft Excel or other programs for further data manipulation.
- **.ac** – AC3D view of the aircraft. AC3D is a 3D graphic format for the description of models, as supported by the AC3D tool.
- **.m** – Geometric input file for the MATLAB solid/wireframe modeler.

After executing the input file with Datcom+ Pro, the output file generated by it quite looks like a collection of tables for different altitudes and mach numbers as shown in Figure 5.2.

```

AUTOMATED STABILITY AND CONTROL METHODS PER APRIL 1976 VERSION OF DATCOM
CHARACTERISTICS AT ANGLE OF ATTACK AND IN SIDESLIP
WING-BODY CONFIGURATION
ENA-01: Flight Conditions, Body, Inertia, Wing

```

FLIGHT CONDITIONS						REFERENCE DIMENSIONS					
MACH NUMBER	ALTITUDE	VELOCITY	PRESSURE	TEMPERATURE	REYNOLDS NUMBER	REF. AREA	REFERENCE LENGTH LONG.	LAT.	MOMENT HORIZ	REF. CENTER VERT	
	M	M/SEC	N/ M**2	DEG K	1/ M	M**2	M	M	M	M	
.040	10.00	13.61	1.0121E+05	288.085	9.2675E+05	.319	.210	1.520	.463	.185	
-----DERIVATIVE (PER DEGREE)-----											
ALPHA	CD	CL	CM	CN	CA	XCP	CLA	CMA	CYB	CNB	CLB
-3.0	.027	-.003	-.0511	-.004	.027	12.429	8.044E-02	-1.969E-03	-1.223E-03	-1.400E-04	-1.401E-04
.0	.030	.248	-.0508	.248	.030	-.205	8.676E-02	2.177E-03			-4.311E-04
1.0	.032	.336	-.0479	.336	.026	-.143	8.890E-02	3.594E-03			-5.330E-04
2.5	.037	.472	-.0409	.473	.017	-.087	9.175E-02	5.808E-03			-6.906E-04
5.0	.050	.706	-.0217	.708	-.012	-.031	9.537E-02	9.593E-03			-9.627E-04
7.5	.068	.949	.0070	.949	-.056	.007	9.821E-02	1.339E-02			-1.244E-03
10.0	.093	1.197	.0452	1.195	-.117	.038	9.047E-02	1.672E-02			-1.533E-03
12.5	.117	1.401	.0906	1.393	-.189	.065	7.146E-02	1.910E-02			-1.769E-03
15.0	.139	1.555	.1407	1.538	-.268	.092	5.145E-02	2.096E-02			-1.947E-03

Figure 5.2: A portion of the output file (.out) for ENA-01

The main output (**.out**) was imported to Matlab to view different parameters and stability derivatives. Figure 5.3 shows the profile of coefficient of lift ($C_{L\alpha}$) and coefficient of drag ($C_{D\alpha}$) due to basic geometry of ENA-01 for different AOA considering the airfoil is in 0.05 and 0.5 mach assuming constant temperature.

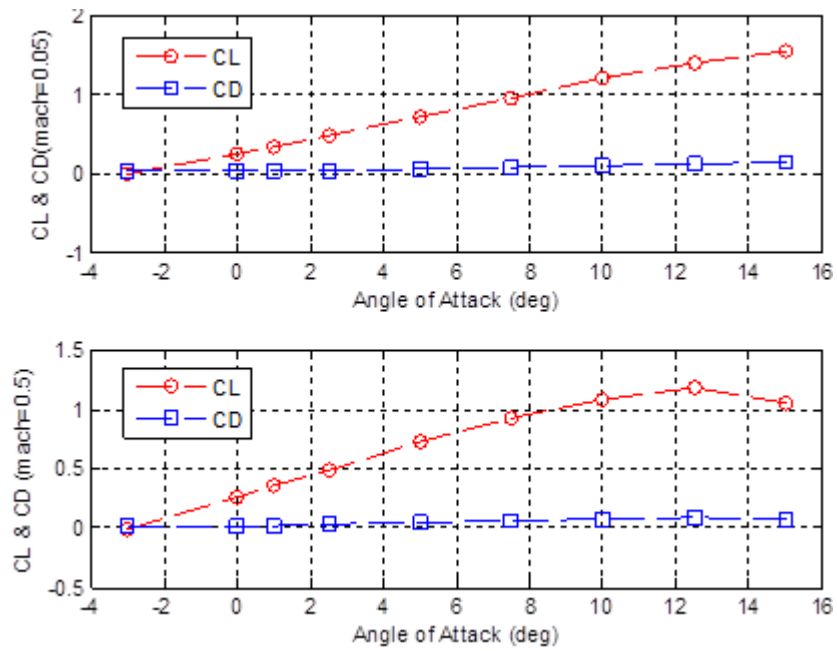


Figure 5.3: Lift and drag coefficient at different AOA

All the coefficients that were extracted from running the Datcom program are placed in Table 5.1.

Table 5.1: Stability and Control Derivatives from Datcom output (for ENA-01)

Lift coefficient due to wing body and horizontal tail
Lift coefficient increment due to elevator deflection
Lift coefficient derivative due to pitch rate per deg
Lift coefficient derivative due to AOA rate per deg
Drag coefficient due to wing body and horizontal tail
Drag coefficient increment due to elevator deflection
Side force coefficient derivative due to sideslip per deg
Side Force coefficient derivative due to roll rate per deg
Side Force coefficient derivative due to yaw rate
Side Force coefficient increment due to plain flap aileron
Side Force coefficient increment due to rudder
Pitch moment coefficient as a function of alpha
Pitch moment coefficient derivative due to AOA rate per deg
Pitch moment coefficient derivative due to pitch rate per deg
Pitch moment coefficient increment due to elevator deflection
Roll moment coefficient derivative due to roll rate
Roll moment coefficient derivative due to sideslip
Roll moment coefficient derivative due to yaw rate per deg
Roll Moment coefficient increment due to aileron deflection
Roll moment coefficient increment due to rudder

A pictorial view of the whole airframe, fuselage and airfoil cross section is presented

in Figure 5.4, Figure 5.5 and Figure 5.6 consecutively. Here station refers the position of the airframe starting from nose.

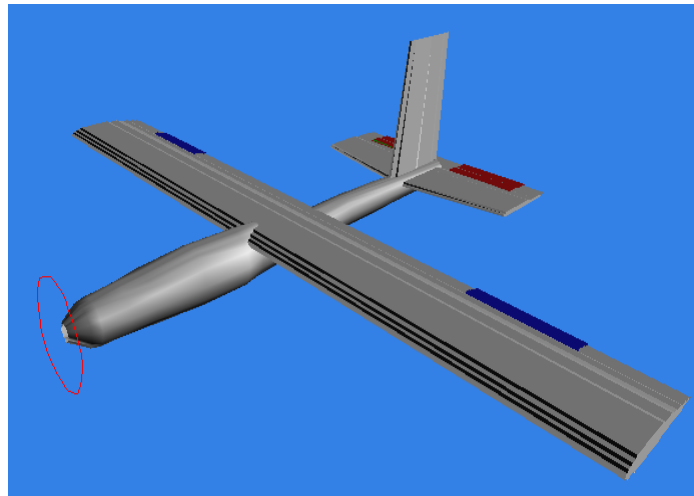


Figure 5.4: ENA-01 airframe in AC3D view (.ac)

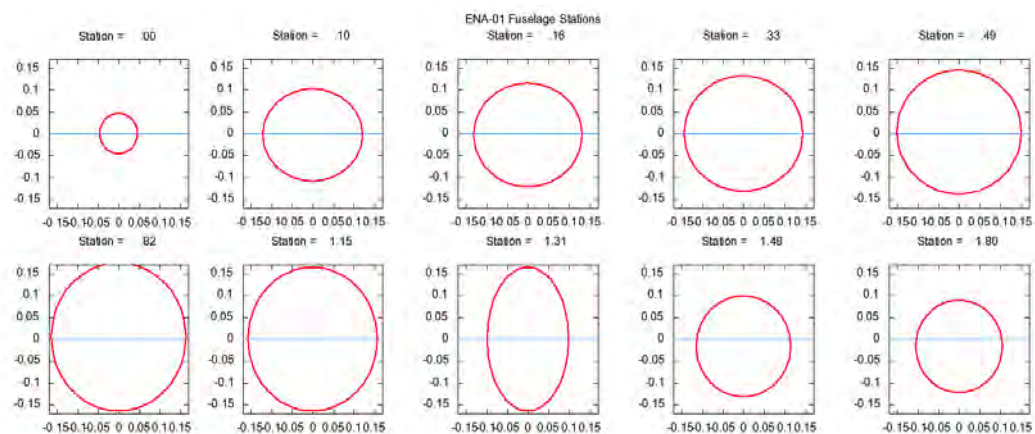


Figure 5.5: Fuselage cross section at different stations

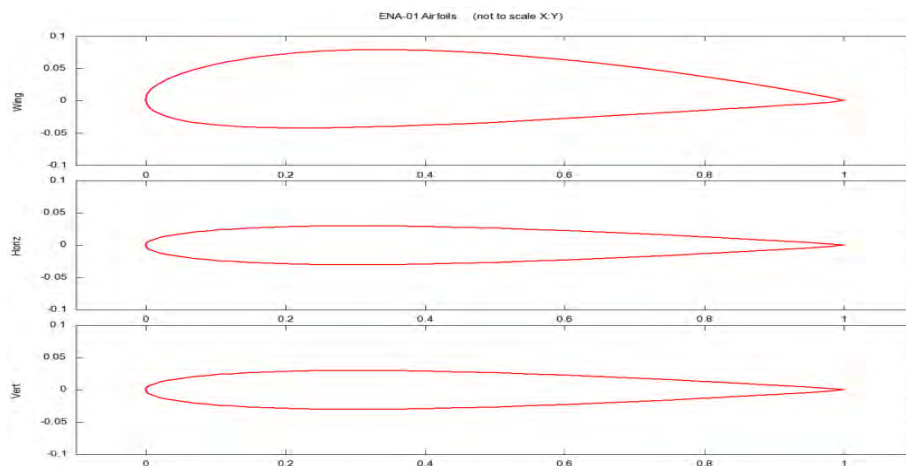


Figure 5.6: Airfoil profiles of wing, horizontal and vertical stabilizer

5.3 Simulink Implementation of ENA-01

Aerospace Blockset of Simulink contains a library of blocks implementing equations of motions. A ‘Three-DOF (Body Axes)’ block was chosen as the starting point for modeling the longitudinal dynamics of ENA-01. As to complete the model for simulation and feed batch data to FlightGear, a conversion block, named as ‘3DoF to 6DoF’ was used. The connection of the aforementioned blocks is shown in Figure 5.7.

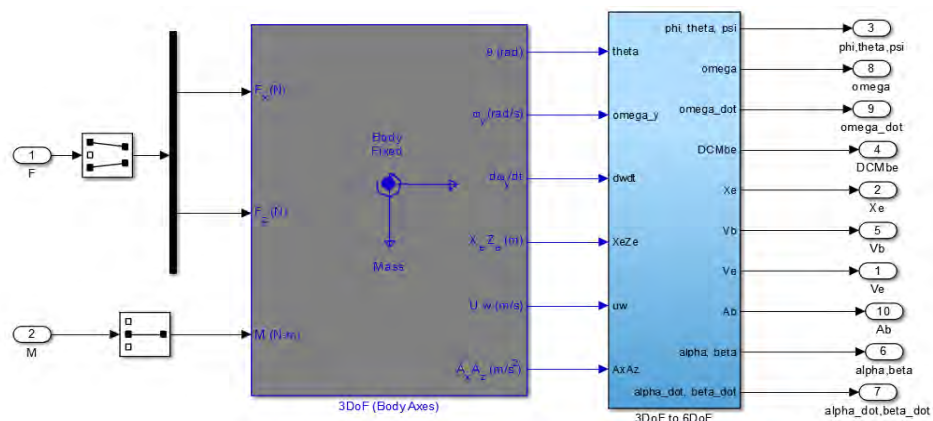


Figure 5.7: Implementing equations of motion

The ‘Digital DATCOM Forces and Moments block’ under the ‘Aerodynamics’ sub library computes aerodynamic forces and moments acting about the center of gravity of ENA-01 using stability derivatives imported from output (.out) file. The effect of elevator deflection was incorporated by an attained ‘Elevator contribution to Force and Moment’ block. Figure 5.8 shows how these are interconnected.

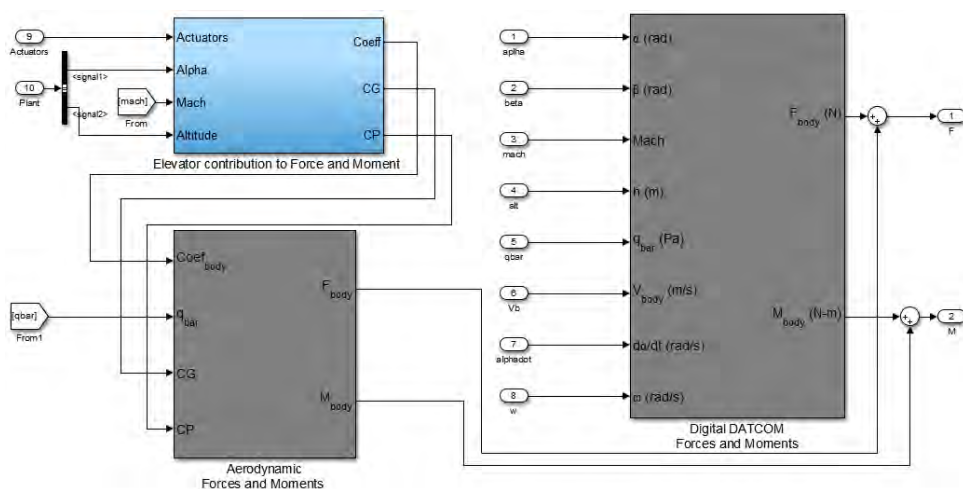


Figure 5.8: Force and moment computation

To calculate gravity forces and moments, a local gravity vector was multiplied by vehicle mass, taking altitude and latitude as input to ‘WGS84 Gravity Model’ block, as shown in Figure 5.9. One thing is important to mention that Direction Cosine Matrix (DCM) was generated inside the ‘3DoF to 6DoF’ block by ‘Euler2DCM’ to keep it mobile for necessary axis conversion.

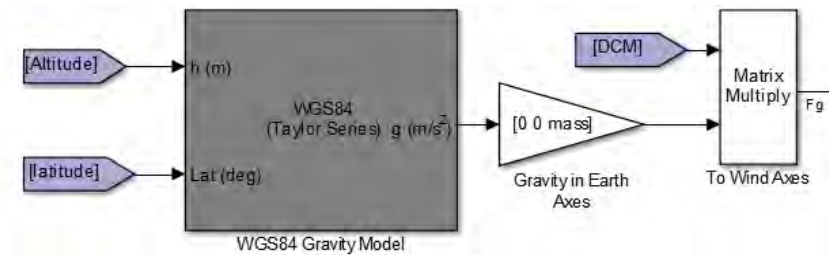


Figure 5.9: Calculation of gravity force

For the purpose of simulating propulsion forces and moments here, a simple lookup table was used to calculate thrust as a function of throttle command, though a brushless dc motor was used for propulsion in ENA-01. Calculation of propulsive force and moment is shown in Figure 5.10. Propulsive moment was assumed absent.

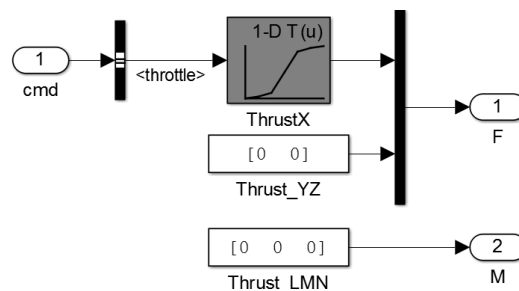


Figure 5.10: Calculation of propulsive force and moment

Now, the inclusion of environmental effect was essential to the model as because airplane performance is largely dependent on the condition in which it would be flown. Fortunately, ‘Environment’ sub-library of Aerospace Blockset has ‘COESA Atmosphere Model’ to imitate 1976 COESA-extended U.S. Standard Atmosphere. Moreover ‘Dryden Wind Turbulence Model’ was also helpful to add artificial turbulence to the aerospace model, as shown in Figure 5.11.

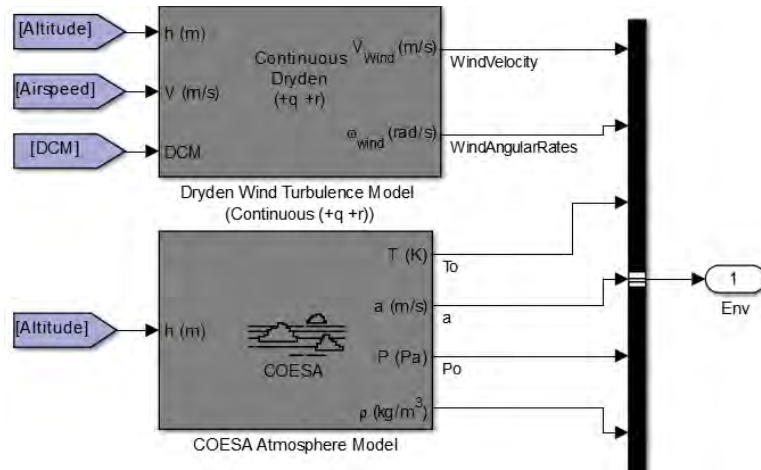


Figure 5.11: Incorporating airplane operating environment

The ‘Nonlinear Second-Order Actuator’ block from the ‘Actuator’ sub-library was included to the model to implement servos for the flight control surfaces, shown in Figure 5.12. As pitch controlling elevator was the only concern for this work, other actuator outputs were blocked (not shown here). It should be noted that the natural frequency and the damping ratio of the actuator were put carefully.

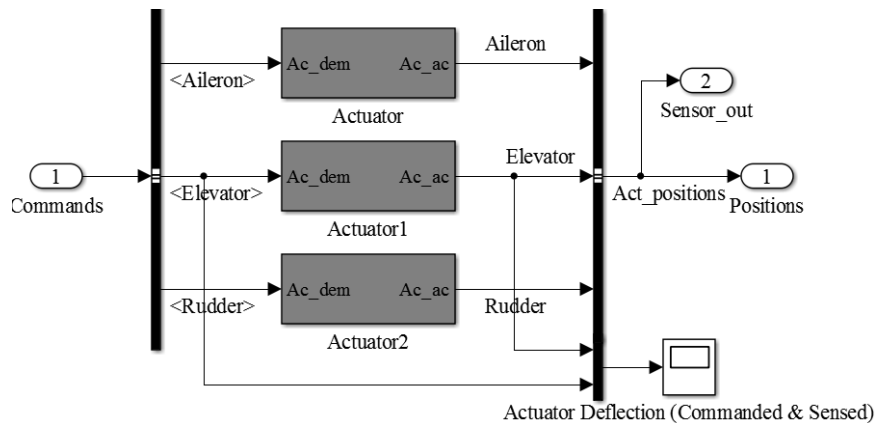


Figure 5.12: Actuators of flight control surfaces

Now, for the control part of this design process, it has to keep in mind that the UAV model in Simulink is only intended for the altitude hold mode. That means ENA-01 will follow the actuator command to ascend or descend to desired altitude as operated and will not collapse or lose its static stability due to any external disturbance. For this reason, it is necessary to have two control loops, one for pitch control and the other one is for altitude control as shown in Figure 5.13.

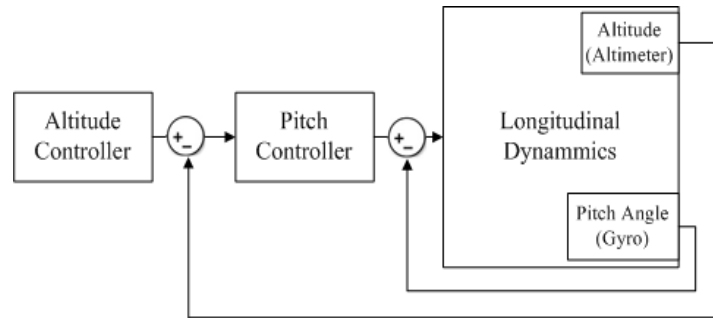


Figure 5.13: Longitudinal controller- inner pitch loop and outer altitude loop

In the Autopilot subsystem of the Simulink model, two ‘PID Controller’s from the ‘Discrete’ library of Simulink were placed to serve this purpose. These were modeled in discrete domain to facilitate the code generation. Though the auto tuning facility of the PID block is quite convenient, an interactive tuning was involved to extract the best result, since the two loops are interdependent.

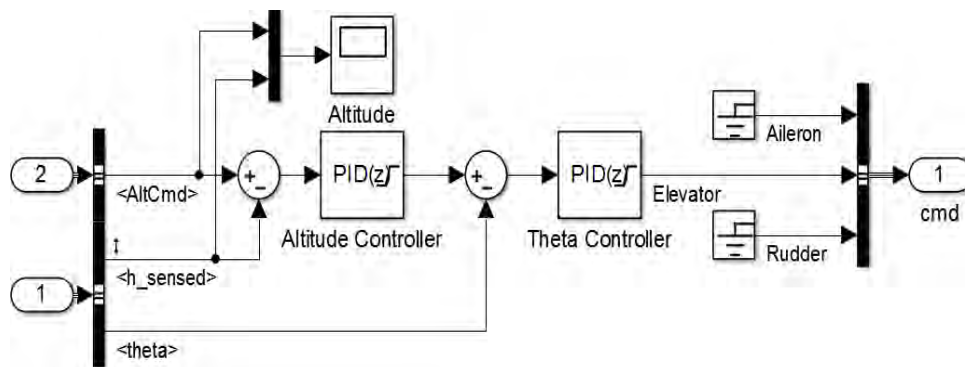


Figure 5.14: Autopilot design using PID controller

Before tuning the PID controllers, the whole model was linearized using ‘Linear Analysis Tool’, defining elevator command and sensed altitude as input and output of linear analysis points. The exact linearization was done after trimming the model at different operating points using snapshot tool covering the whole flight envelop. A portion of the trimmed output is shown in Figure 5.15. The tuning window of the altitude controller with performance parameters is shown in Figure 5.16. It shows the block response, before and after tuning, in respect of a step response. The theta controller is also tuned in a similar way.

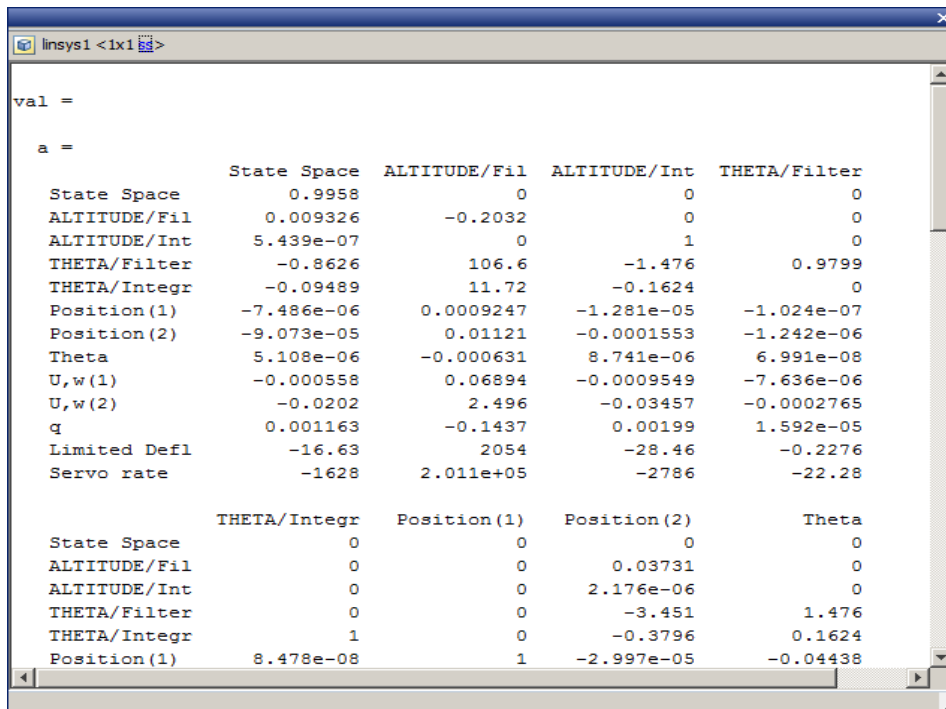


Figure 5.15: A portion of the state space trimmed output

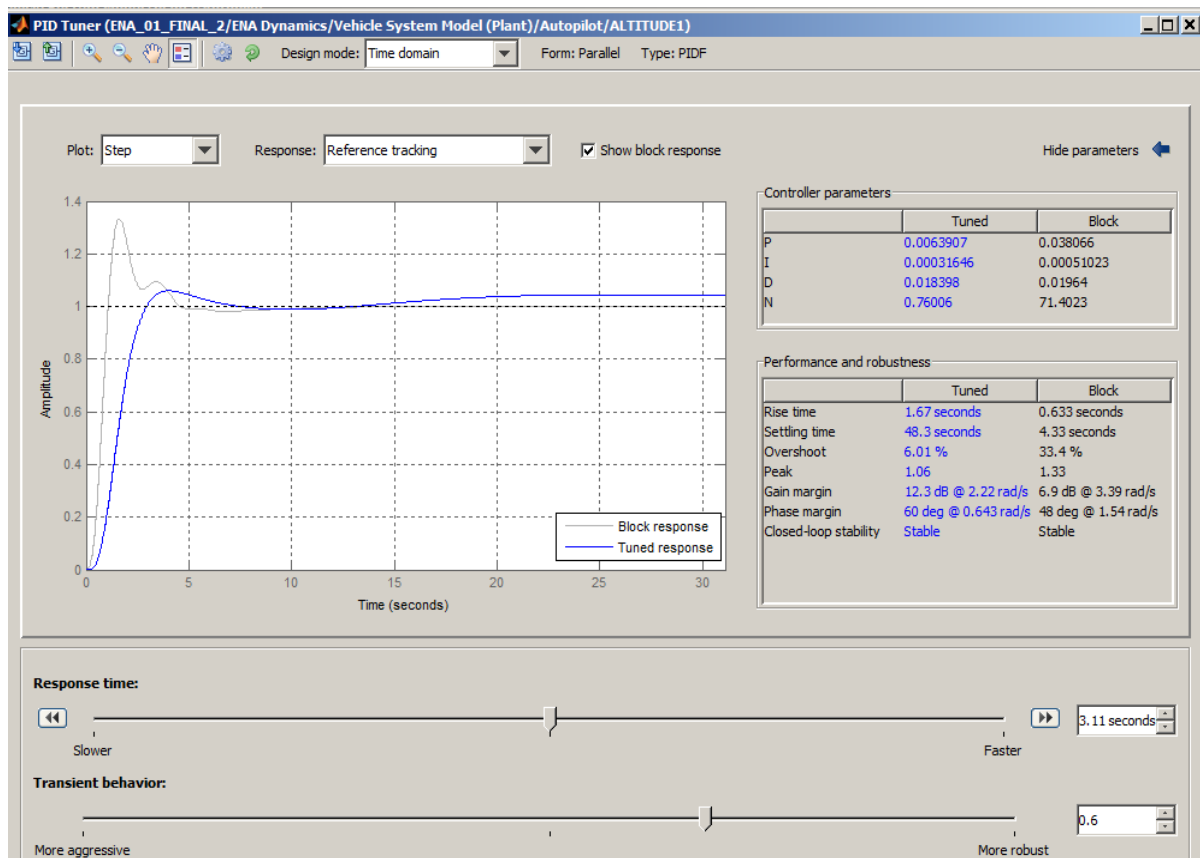


Figure 5.16: Tuning of the altitude controller

After setting and tuning up all the parameters in the base and model workspace, an

actuation command to elevate the airplane 100 meter from 300 meter is shown in Figure 5.17. It demonstrates that the vehicle is quite stable in the pitch plane and can follow a satisfactory climb rate.

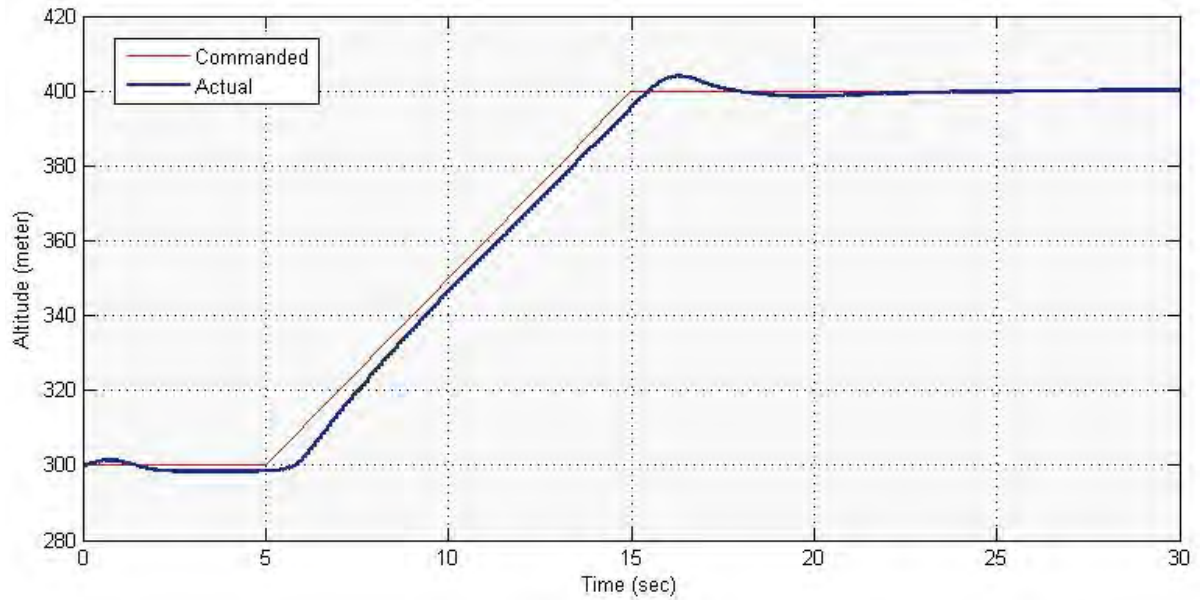


Figure 5.17: Altitude command and response

After inserting a turbulence of 30 meter/second value from the Dryden Wind Turbulence Model block, it is observed that the controller still gives an acceptable response.

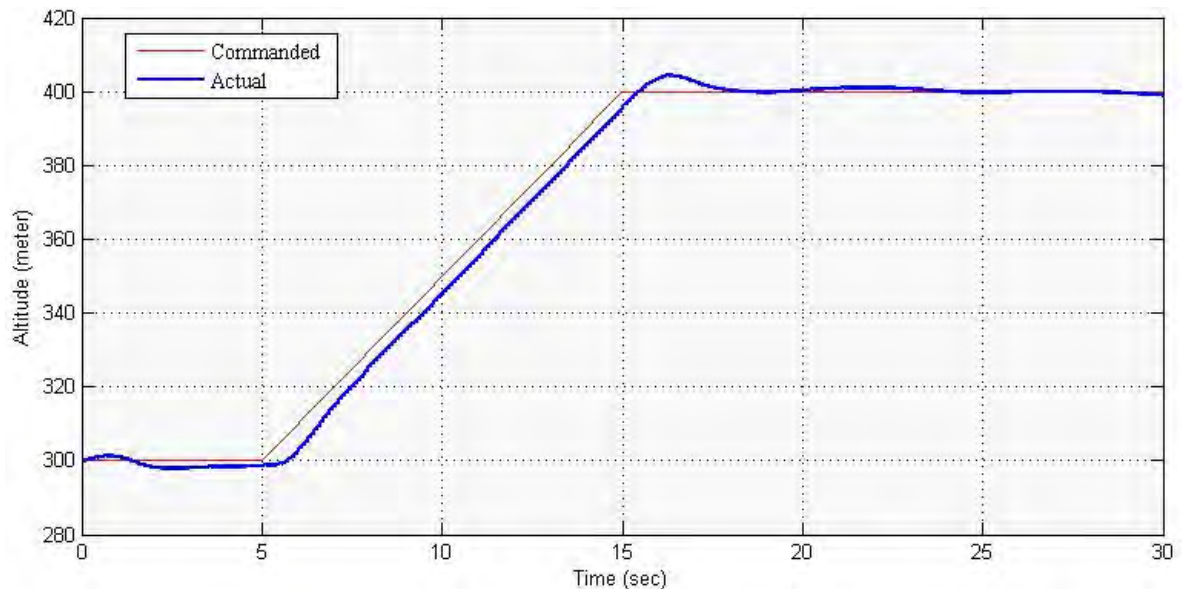


Figure 5.18: Altitude command and response with turbulence

5.4 Visualization in FlightGear

By setting up a script with compatible FlightGear version, the simulation can be easily visualized in real time environment, as shown in Figure 5.19.



Figure 5.19: FlightGear data feed setup and visualization

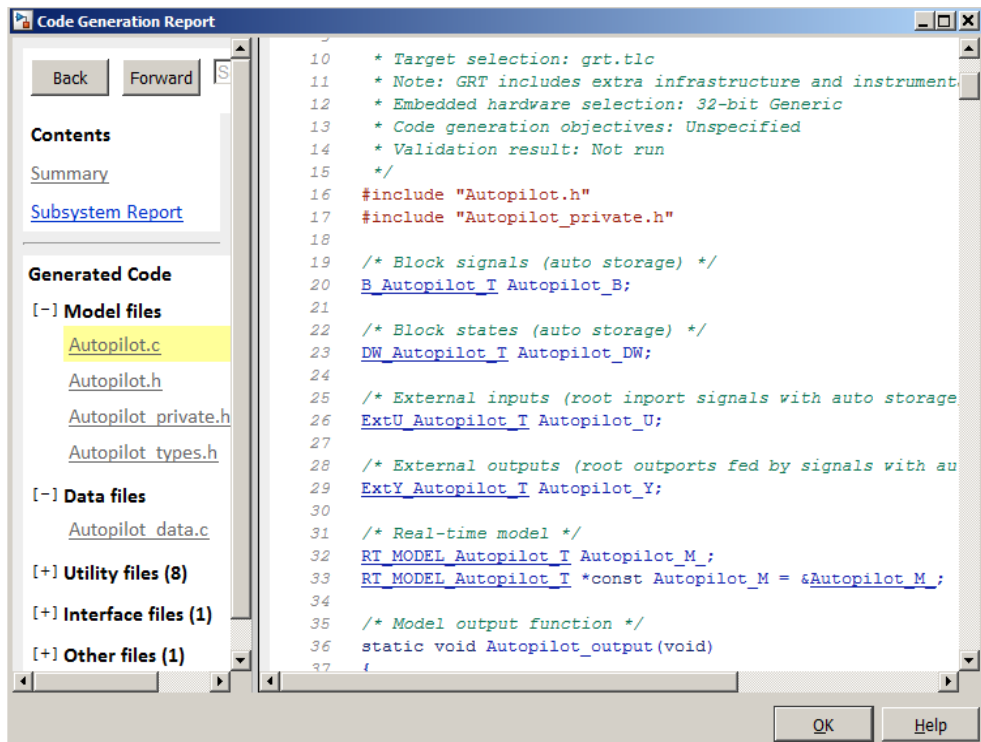
The FlightGear version 0.9.10 was used in this work. While running this software, it is recommended to put the computer on minimum load. Proper configuration of destination IP address, destination port and sample time is essential.

5.5 Microcontroller Code Generation

The MATLAB code generation tools are capable of generating embedded C/C++ code optimized for specific hardware directly from Simulink models. This process effectively avoids the possible introduction of manually coded errors and increase the reliability of the code and consistency between the code implementation and Simulink model.

The pitch controller autopilot section of our model can be easily implanted to quite a number of microcontrollers available in market. Our target hardware was Texas Instrument C2000. It is a family of popular 32 bit microcontrollers, has interactive development environment that can edit generated code and work as a debugger. The code generation in Simulink is easy, just a right click on the subsystem, then enter to 'C/C++ Code' to 'Build

This Subsystem'. A portion of the generated code is shown in Figure 5.20, viewed from the 'Code Generation Report' window.



The screenshot shows a window titled "Code Generation Report" with a sidebar on the left and a main text area on the right. The sidebar contains a "Contents" section with links for "Summary" and "Subsystem Report", and a "Generated Code" section with sub-sections for "Model files", "Data files", "Utility files (8)", "Interface files (1)", and "Other files (1)". The "Autopilot.c" file is highlighted under "Model files". The main text area displays C code with line numbers 10 through 37. The code includes comments about target selection, hardware selection, and code generation objectives, followed by include statements for "Autopilot.h" and "Autopilot_private.h", and declarations for block signals, states, external inputs, and outputs. It also shows a real-time model declaration and a static void function declaration for "Autopilot_output".

```
10  * Target selection: grt.tlc
11  * Note: GRT includes extra infrastructure and instrument
12  * Embedded hardware selection: 32-bit Generic
13  * Code generation objectives: Unspecified
14  * Validation result: Not run
15  */
16  #include "Autopilot.h"
17  #include "Autopilot_private.h"
18
19  /* Block signals (auto storage) */
20  B_Autopilot_T Autopilot_B;
21
22  /* Block states (auto storage) */
23  DW_Autopilot_T Autopilot_DW;
24
25  /* External inputs (root inport signals with auto storage) */
26  ExtU_Autopilot_T Autopilot_U;
27
28  /* External outputs (root outports fed by signals with au
29  ExtY_Autopilot_T Autopilot_Y;
30
31  /* Real-time model */
32  RT_MODEL_Autopilot_T Autopilot_M;
33  RT_MODEL_Autopilot_T *const Autopilot_M = &Autopilot_M;
34
35  /* Model output function */
36  static void Autopilot_output(void)
37  {
```

Figure 5.20: Generated C code for 'Autopilot' subsystem (pitch controller)

CHAPTER 6

ECONOMIC EVALUATION

6.1 Introduction

Flight control design is a complex and tedious work. It needs to cover all aspects of airplane operation and must be economical, not only from functional perspective, but also from maintenance. This research work is a part of this whole process as it only includes the design of pitch controller for a single mode. In the following section, a cost estimation to implement our design in the UAV is presented, with detail pricing of individual component. And next to that, with a similar control design process, a simple cost assessment is done for a civil aircraft carrier.

6.2 Cost for Pitch Controller Installation in ENA-01

The components that are needed for pitch controller for the UAV is shown in Figure 6.1.

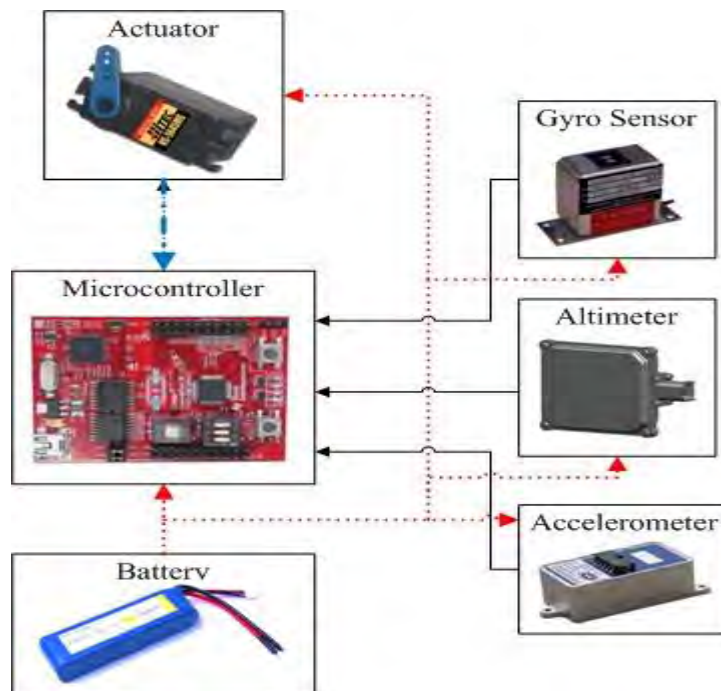


Figure 6.1: Proposed onboard components of pitch controller for ENA-01

A cost assessment with individual product description to implement the controller is introduced in Table 6.1.

Table 6.1: Price detail for ENA-01 pitch controller

Component	Product Detail	Price (USD)
Microcontroller	LAUNCHXL-F28027-C2000 Piccolo LaunchPad [47]	18.50
Altimeter	SmartMicro Radar Altimeter [48]	34.95
Gyro and Accelerometer	Triple Axis Accelerometer & Gyro - MPU-6050 [49]	49.15
Battery	Hyperion G3 CX7.4v 2S 4000mah 25C/45C Lipo [50]	40.95
Elevator Servo	Hitec HS-5645MG Metal Gear Digital Servo [51]	54.95
Speed Controller	HobbyWing 40Amp OPTO Brushless Motor ESC Speed Controller [52]	29.75

Both propulsion and electrical power for a carrier aircraft come from engine, in expense of combustion. On contrary, in UAV, the only power source is battery that provides thrust through speed controller, as well as power to the actuator. This actuator for a particular airplane is dependent on the load and actuation type. However, their prices are placed in the table, but not to be considered as a part of the control architecture.

Apart from taking the cost of the software Datcom+ Pro, wiring and some data conversion process in consideration, the pitch controller will require approximately 100 US dollars. It has been made sure that all these components listed in Table 6.1 are electronically compatible.

6.3 Estimating Cost for Carrier Airplane

Wide body carriers have cruise flights at 10 kilometers altitude to achieve fuel efficient operation, whereas short haul airplanes fly on around 4 kilometers height. The measurement of altitude by radio altimeter is quite erroneous in that region. Again radio altimeter is essential for crew to have correct idea about ground clearance. That's why pitch controller in carrier airplanes must have interface with both types of altimeter. An estimation of cost to implant a pitch controller in a short range carrier is shown in Table 6.2.

Table 6.2: Price estimation for a manned aircraft

Component	Price (USD)
Microcontroller	18.50
Barometric Altimeter	60.00
Radio Altimeter	40.00
Gyroscope	50.00
Accelerometer	40.00

From the table, it can be said that the expenditure is around 200 US dollars, considering wider margin of operation of the respective items compared to the UAV. However, this evaluation is just an approximation. The scope, capability, accuracy and compatibility of these items are to be ensured and evaluated with hardware in the loop test and test flights.

CHAPTER 7

CONCLUSION AND SUGGESTION FOR FUTURE WORK

7.1 Conclusion

This thesis established a workflow to develop a pitch controller for a UAV as a model airplane. It set off by constructing the airframe of the UAV and computing the aerodynamic characteristic to verify it's natural stability. Then with the help of stability parameters, it went along with the process of designing and tuning PID controller to follow pilot command only on pitch axis, ensuring reliability of airplane operation in adverse condition, for a certain configuration of flight. Besides, a complete simulation environment made it easy to visualize accuracy of the controller.

Personally my achievement in this thesis is to learn how to construct a UAV, how to employ airplane dynamics in Simulink and finally how to develop a controller for it.

7.2 Suggestion for Future Work

This thesis work shows a simple way to design a pitch controller for a UAV, approaching at the end of execution level. In a similar way, controller for lateral dynamics can also designed for a wide range of airplanes, may be with more robust and faster control design tool, like dynamic inversion, neuro adaptive design, kalman filtering etc. And finally, combining pitch and roll controller, a complete autopilot can be designed. Evidently, flight tests are essential to comprehend the usefulness of the design.

APPENDIX I: DATCOM

Introduction:

The United States Air Force Stability and Control Digital DATCOM is a computer program that implements the methods contained in the USAF Stability and Control DATCOM to calculate the static stability, control and dynamic derivative characteristics of fixed-wing aircraft. Digital DATCOM requires an input file containing a geometric description of an aircraft, and outputs its corresponding dimensionless stability derivatives according to the specified flight conditions. The values obtained can be used to calculate meaningful aspects of flight dynamics.

In February 1976, work commenced to automate the methods contained in the USAF Stability and Control DATCOM. The work was performed by the McDonnell Douglas Corporation under contract with the United States Air Force in conjunction with engineers at the Air Force Flight Dynamics Laboratory in Wright-Patterson Air Force Base. Implementation of the Digital DATCOM concluded in November 1978. The program is written in FORTRAN IV and has since been updated; however, the core of the program remains the same.

A report was published, separated into three volumes, which explains the use of Digital DATCOM. The report consists of

Volume I: User's Manual

Volume II: Implementation of DATCOM Methods

Volume III: Plot Module

Inputs:

Section 3 of the USAF Digital DATCOM Manual Volume I defines the inputs available for modeling an aircraft. The inputs are categorized by namelists to facilitate reading the file into FORTRAN.

Flight conditions and options:

The FLTCON Namelist describes the flight conditions for the case. A maximum of 400 Mach-altitude combinations can be run at once, with up to 20 angles of attack for each combination. The user can specify whether the Mach number and altitude varies together, the Mach number varies at a constant altitude, or the altitude varies at a constant Mach number. Both subsonic and supersonic analysis can be run in Digital DATCOM.

The OPTINS Namelist defines the reference parameters for the aircraft. The theoretical

wing area, mean aerodynamic chord, and wing span are input along with a parameter defining the surface roughness of the aircraft.

Synthesis parameters:

The SYNTHS Namelist allows the user to define the positions of the center of gravity and apexes of the wings. The X- and Z- coordinates are needed for the wing, horizontal tail, and vertical tail in order for the aircraft to be synthesized correctly. DATCOM does not require that the origin for the aircraft has to be the nose of the aircraft; any arbitrary point will do, but all of the dimensions need to be referenced from that point. Incidence angles can also be added to the wing and horizontal tail.

Body parameters:

The BODY Namelist defines the shape of the body. Digital DATCOM assumes an axisymmetrical shape for the body. Up to 20 stations can be specified with the fuselage half-width, upper coordinate and lower coordinate being defined at each station. For supersonic analysis, additional parameters can be input.

Wing, Horizontal and Vertical Tail parameters:

The WGPLNF, HTPLNF and VTPLNF Namelists define the wing, horizontal tail and vertical tail, respectively. The basic parameters such as root chord, tip chord, half-span, twist, dihedral and sweep are input. Digital DATCOM also accepts wing planforms which change geometry along the span such as the F4 Phantom II which had 15 degrees of outboard dihedral. Canards can also be analyzed in Digital DATCOM. The canard must be specified as the forward lifting surface (i.e. wing) and the wing as the aft lift surface. For airfoil designations, most traditional NACA 4-, 5-, and 6- airfoils can be specified in Digital DATCOM. Additionally, custom airfoils can be input using the appropriate namelists. Also, twin vertical tails can be designated in Digital DATCOM, but not twin booms.

High Lift and Control Devices:

Using the SYMFLP and ASYFLP Namelists, flaps, elevators, and ailerons can be defined. Digital DATCOM allows a multitude of flap types including plain, single-slotted, and fowler flaps. Up to 9 flap deflections can be analyzed at each Mach-altitude combination. Unfortunately, the rudder is not implemented in Digital DATCOM. Digital DATCOM also offers an automated aircraft TRIM function which calculates elevator

deflections needed to trim the aircraft.

Output:

Digital DATCOM produces a copious amount of data for the relatively small amount of inputs it requires. By default, only the data for the aircraft is output, but additional configurations can be output:

Body alone

Wing alone

Horizontal tail alone

Vertical tail alone

Wing-Body Configuration

Body-Horizontal Tail Configuration

Body-Vertical Tail Configuration

Wing-Body-Horizontal Tail Configuration

Wing-Body-Vertical Tail Configuration

Wing-Body-Horizontal Tail-Vertical Tail Configuration

For each configuration, stability coefficients and derivatives are output at each angle of attack specified. The details of this output are defined in Section 6 of the USAF Digital DATCOM Manual Volume I. The basic output includes:

C_L - Lift Coefficient

C_D - Drag Coefficient

C_m - Pitching Moment Coefficient

C_N - Normal Force Coefficient

C_A - Axial Force Coefficient

$C_{L\alpha}$ - Lift Curve Slope (Derivative of Lift Coefficient with respect to angle of attack)

$C_{m\alpha}$ - Pitching Moment Curve Slope (derivative of Pitching Moment Coefficient with respect to angle of attack)

$C_{Y\beta}$ - Derivative of side-force coefficient with respect to sideslip angle

$C_{n\beta}$ - Derivative of yawing-moment coefficient with respect to sideslip angle

$C_{l\beta}$ - Derivative of rolling-moment coefficient with respect to sideslip angle

For complete aircraft configurations, downwash data is also included.

When compared with modern methods of computational fluid dynamics, Digital

DATCOM may seem antiquated. However, in its day, the program was an advanced estimation tool, and certainly much faster than plowing through pages and pages of engineering texts. Digital DATCOM is no longer supported by the USAF and is now public domain software.

Limitations:

Inlets, external stores, and other protuberances cannot be input because Digital DATCOM analyzes the fuselage as a body of revolution. The simplification affects the coefficient of drag for the aircraft. Dynamic derivatives are not output for aircraft that have wings that are not straight-tapered or have leading edge extensions. This problem can be overcome by using experimental data for the wing-body (using non-straight tapered wing). There is no method to input twin vertical tails mounted on the fuselage, although there is a method for H-Tails. This problem can be addressed by approximating the twin vertical tails as a single equivalent vertical tail mounted to the fuselage. Digital DATCOM cannot provide outputs for the control derivatives with regard to the rudder control surface. According to the manual, there is no any input parameters which define the geometry of rudder.

APPENDIX II: Datcom input file (.dcm)

```

*   Aircraft ENA-01 UAV
*   Author: Nafis Kabir
*   M. Sc. Thesis
*   Bangladesh University of Engineering & Technology

DIM M
DERIV DEG
DAMP

CASEID ENA-01: Flight Conditions, Body, Inertia, Wing
$FLTCON   WT=3.3,
           #weight in pounds

           LOOP=2.0,
           #vary altitude and mach number together

           NMACH=10.0,      MACH(1)=0.02,0.04,0.06,0.08,0.1,0.12,0.14,0.16,0.18,0.20,
           #defining number of machs and their values

           NALT=10.0,      ALT(1)=10.0,50.0,100.0,150.0,200.0,250.0,300.0,350.0,400.0,450.0,
           #defining number of altitudes and their value (in meter)

           NALPHA=9.0,     ALSCHD(1)=-3.0,0.0,1.0,2.5,5.0,7.5,10.0,12.5,15.0$
           #defining number of altitudes and their value (in degree)

$OPTINS   SREF=0.3192,
           #wing surface area (in square meter)

           CBAR=0.21,
           #wing mean aerodynamic chord (in meter)

           BLREF=1.52$
           #wing span (in meter)

$SYNTHS   XCG=0.4625,ZCG=0.185,
           #CG position from nose and landing gear touchdown point (in meter)

           XW=0.41,ZW=0.032,
           #wing position from nose and landing gear touchdown point (in meter)

           ALIW= 1.2, VERTUP=.TRUE.,
           #wing incident angle (in degree) and vertical stabilizer orientation

           XH=0.88, ZH=0.0105, ALIH=0.5,
           #horizontal stabilizer position from nose and landing gear touchdown point (in
meter) and its incident angle

           XV=0.86, ZV= 0.014$
           #vertical stabilizer position from nose and landing gear touchdown point

$BODY     NX=14.0,
           X(1)=0.05,0.08,0.1,0.15,0.2,0.3,0.4,0.45,0.5,0.6,0.7,0.8,0.9,1.04,
S(1)=0.00053,0.0038,0.0050,0.0061,0.0066,0.0078,0.0075,0.045,0.0038,0.0032,0.0028,0.0026,0.00
21,0.0018,
           P(1)=0.9,0.23,0.25,0.27,0.34,0.43,0.40,0.3,0.3,0.27,0.24,0.22,0.19,0.17,
R(1)=0.014,0.037,0.04,0.044,0.046,0.05,0.048,0.03,0.035,0.032,0.03,0.029,0.026,0.024,
           ZL(1)=-0.014,-0.033,-0.037,-0.04,-0.042,-0.05,-0.05,-0.05,-0.04,-0.03,-0.02,-
0.018,-0.015,-0.014,
ZU(1)=0.014,0.031,0.035,0.04,0.044,0.053,0.05,0.05,0.03,0.02,0.02,0.018,0.015,0.014$
           #fuselage stations and their half lengths

$INERTA   IXX=0.9, IYY=1.3, IZZ=1.7, IXZ=0.0,
           #moment and product of inertias

           ACTYPE=1.0$
           #aircraft type: light single engine

NACA-W-4-2412
           #wing aerofoil type

```

```

$WGPLNF   CHRDR=0.21,CHRDTF=0.21,
           #wing chord length in fuselage center line and wing tip (in meter)

           TYPE=1.0,
           #type of planform - 1.0=straight tapered planform

           SSPN=0.76,
           #distance from fuselage center line to wing tip (in meter)

           SSPNE=0.7125$
           #distance from fuselage to wing tip (in meter)

SAVE
NEXT CASE

CASEID ENA-01: Ailerons
$ASYFLP   STYPE=4.0,
           #aileron type - 4 = plain flap

           SPANFI=0.41, SPANFO=0.612,
           #aileron inboard and outboard distance from the fuselage center line

           CHRDFI=0.0303, CHRDFO=0.0303,
           #chord in aileron inboard and outboard sections

           NDELTA=8.0,
           DELTAL(1)=-20.0,-15.0,-10.0,-5.0,0.0,5.0,10.0,15.0,
           DELTAR(1)=15.0,10.0,5.0,0.0,-5.0,-10.0,-15.0,-20.0$
           #number of aileron deflections and their values for left and right ailerons

SAVE
NEXT CASE

CASEID ENA-01: Horizontal Tail, Vertical Tail, Elevator

NACA-H-4-0006
           #horizontal stabilizer aerofoil type

$HTPLNF   CHRDR=0.218,CHRDTF=0.18,
           #horizontal stabilizer chord length in fuselage center line and wing tip (in
meter)

           SSPN=0.27,
           #distance from fuselage center line to horizontal stabilizer tip (in meter)

           SSPNE=0.236,
           #distance from fuselage to horizontal stabilizer tip (in meter)

           SAVSI=10.0,CHSTAT=0.0,
           #sweep angle (in degree) and the position where it is measured

           TWISTA=0.0,DHDADI=0.0,
           #washout angle, dihedral angle

           TYPE=1.0$
           #type of planform - 1.0=straight tapered planform

NACA-V-4-0006
           #vertical stabilizer aerofoil type

$VTPLNF   CHRDR=0.184,CHRDTF=0.147,
           #vertical stabilizer chord length in fuselage center line and in tip (in meter)

           SSPN=0.28,
           #distance from fuselage center line to vertical stabilizer tip (in meter)

           SSPNE=0.262,
           #distance from fuselage to vertical stabilizer tip (in meter)

           SAVSI=10.0,CHSTAT=0.0,
           #sweep angle (in degree) and the position where it is measured

           TYPE=1.0$
           #type of planform - 1.0=straight tapered planform

$SYMFLP   FTYPE=1.0,NTYPE=1.0,

```

```

SPANFI=0.05,SPANFO=0.219,
#elevator position in horizontal stabilizer

CHRDFI=0.058,   CHRDFO=0.058,
#chord in elevator inboard and outboard sections

NDELTA=9.0,      DELTA(1)=-28.0,-20.0,-10.0,-5.0,0.0,7.5,15.0,20.0,23.0$
#defining number of elevator deflections (in degree) and their value

SAVE
NEXT CASE

CASEID ENA-01: Engine      eng=eng_io320      prop=prop_Clark_Y7570
$PROPWR  AIETLF=2.0,
# angle of incidence of engine thrust (in degrees)

NENGSF=1.0,
#number of propeller

THSTCP=0.0,
#thrust coefficient

PHALOC=0.04,YP=0.0,PHVLOC=0.0,
#location of propeller hub

NOPBPE=2.0,PRPRAD=0.085,BAPR75=2.0,ENGFCF=0.8$
#number of blades, propeller radius, blade angle, efficiency

SAVE
NEXT CASE

CASEID ENA-01: Second Power setting
$PROPWR THSTCP=0.01$
SAVE
NEXT CASE

CASEID ENA-01: Third Power setting
$PROPWR THSTCP=0.02255$
SAVE
NEXT CASE

CASEID ENA-01: Fourth Power setting
$PROPWR THSTCP=0.03$

DAMP
BUILD
PLOT
NEXT CASE

```

Bibliography

- [1] Wright, O., Kelly, F.C., (1988) *How We Invented the Airplane: An Illustrated History*, Dover Publications, New York.
- [2] Moir, I., Seabridge, A., “The Design and Development Process” in *Design and Development of Aircraft Systems*, 2nd ed., AIAA Education Series, Wiley Press, 2012.
- [3] Grant R. G., (2007) *Flight: The Complete History*, reprint ed., DK Publishing.
- [4] Collinson, R.P.G., “Fly-by-Wire Flight Control” in *Computing & Control Engineering Journal*, Vol: 10, Issue: 4, Aug. 2002, pp 141-152.
- [5] Dennis, R.W., Hills, A.D., “A Fault Tolerant Fly by Wire System for Maintenance Free Applications” in *IEEE/AIAA/NASA 9th Digital Avionics Systems Conference Proceeding*, Virginia, Oct.1990, pp 11–20.
- [6] Sundberg, G.R., “Civil Air Transport: A Fresh Look at Power-by-Wire and Fly-by-Light” in *Proceedings of the IEEE National Aerospace and Electronics Conference*, Ohio, May 1990, pp 1365–1368.
- [7] Todd, J.R., Hay, J.A., Brennan, M.E., “Integrating Fly-by-Light Systems” in *Proceedings of the IEEE/AIAA 11th Digital Avionics Systems Conference*, Washington, Oct.1992, pp 411–416.
- [8] Stengel, R.F., “Toward Intelligent Flight Control” in *IEEE Transactions on Systems, Man and Cybernetics*, Vol:23, Issue: 6, Aug. 2002, pp 1699–1717.
- [9] Liu, X., Wu, Y., Shi, J., Zhang, W., “Adaptive Fault-Tolerant Flight Control System Design Using Neural Networks” in *IEEE International Conference on Industrial Technology*, Chengdu, Apr. 2008, pp 1–5.
- [10] Boskovic, J. D., Mehra, R. K., “A Multiple Model-Based Reconfigurable Flight Control System Design” in *Proceedings of the 37th IEEE Conference on Decision and Control*, Vol:4, Florida, Dec. 1998, pp 4503 – 4508.
- [11] Pratt, R. W., “Ground and Flight Testing of Digital Flight Control Systems” in *Flight Control Systems*, AIAA Series on Progress in Astronautics and Aeronautics, May 2000.
- [12] Owens D. B., Cox D. E., Morelli E. A., “Development of a Low-Cost Sub-Scale Aircraft for Flight Research: The FASER Project” in *25th AIAA Aerodynamic Measurement Technology and Ground Testing Conference*, California, Jun. 2006.

- [13] Jordan, T. L., Bailey, R. M., "NASA Langley's AirSTAR Testbed: A Subscale Flight Test Capability for Flight Dynamics and Control System Experiments" in *AIAA Guidance, Navigation and Control Conference and Exhibit*, Virginia, Aug. 2008.
- [14] Jordan, T.L., Langford, W.M., Hill, J.S., "Airborne Subscale Transport Aircraft Research Testbed, Aircraft Model Development", in *AIAA Guidance, Navigation, and Control Conference*, Washington, DC, Nov. 2005.
- [15] Hoak, D. E., *et al.*, "The USAF Stability and Control DATCOM," in *Air Force Wright Aeronautical Laboratories Technical Report, AFWAL-TR-83-3048*, Oct. 1960 (Revised 1978).
- [16] Williams, J. E., Vukelich, S. R., "The USAF Stability and Control Digital Datcom", in *United States Air Force Flight Dynamics Laboratory Technical Report AFFDL-TR-79-3032*, McDonnell Douglas Astronautics Company, Missouri, Apr. 1979.
- [17] Datcom+ & Datcom+ Pro by Bill Galbraith
<http://www.holycows.net/Datcom/4973.html>
- [18] USAF Stability and Control Datcom (Data Compendium) in Public Domain Aeronautical Software website
<http://www.pdas.com/datcomDescription.html>
- [19] Blake, W. B. "Prediction of Fighter Aircraft Dynamic Derivatives Using Digital Datcom," *AIAA 3rd Applied Aerodynamics Conference, AIAA-1985-4070*, Colorado, Oct. 1985.
- [20] The Mathworks, Inc. "Model-Based Design of a New Light-weight Aircraft," *AIAA Modeling and Simulation Technologies Conference and Exhibit, AIAA-2007-6371*, South Carolina, Aug. 2007.
- [21] Hsu, C. W. *et al.*, "Using Datcom Method to Analyze Unmanned Aerial Vehicle". AASRC/CCAS Joint Conference, Changhua, 2006.
- [22] Simulink Product page on the MathWorks website.
www.mathworks.com/products/simulink
- [23] Reedy, J., Lunzman, S., "Model Based Design Accelerates the Development of Mechanical Locomotive Controls" in *SAE Commercial Vehicle Engineering Congress*, Oct. 2010.
- [24] Aerospace Blockset Product page on the MathWorks website.
www.mathworks.com/products/aeroblks

- [25] Official page of FlightGear Flight Simulator
<http://www.flightgear.org/>
- [26] FlightGear Simulator page in Wikipedia
<http://en.wikipedia.org/wiki/FlightGear>
- [27] Kimberlin, R.D., (2003) *Flight Testing of Fixed-Wing Aircraft*, AIAA Education Series, Virginia, Chaps 4,15,21.
- [28] Babka, D. W., “Flight Testing in a Simulation Based Environment” B. Sc. Engineering Thesis, Department of Aerospace Engineering, California Polytechnic University, California, 2011.
- [29] List of open publications in official website of FAA
http://www.faa.gov/regulations_policies/handbooks_manuals
- [30] List of open publications in official website of EASA
<http://www.easa.europa.eu/rulemaking/technical-publications.php>
- [31] Kermode, A. C., (2012), *Mechanics of Flight*, 12th ed., Pearson Education.
- [32] Pallett, E. H. J., (1998) *Aircraft Electrical Systems*, 3rd ed., Prentice Hall.
- [33] Pallett, E. H. J., (1992) *Aircraft Instruments and Integrated Systems*, Prentice Hall.
- [34] Pallett, E. H. J., Coyle, S., (1993) *Automatic Flight Control*, 4th ed., Wiley-Blackwell Publications.
- [35] Dingle, L., Tooley, M., (2006) *Aircraft Engineering Principles*, reprint ed., Elsevier Butterworth-Heinemann Publications.
- [36] Tooley, M., Wyatt D., (2009) *Aircraft Electrical and Electronic Systems: Principles, Maintenance and Operation*, Elsevier Butterworth-Heinemann Publications.
- [37] Tooley, M., Wyatt D., (2007) *Aircraft Communications and Navigation Systems: Principles, Operation and Maintenance*, Elsevier Butterworth-Heinemann Publications.
- [38] “Pilot’s Handbook of Aeronautical Knowledge” - *Federal Aviation Administration Handbook, FAA-H-8083-25A*, United States Department of Transportation, Oklahoma, 2007.

- [39] “Aviation Maintenance Technician Handbook – Airframe”, *Federal Aviation Administration Handbook, FAA-H-8083-31*, United States Department of Transportation.
- [40] Roskam J., *Airplane Flight Dynamics and Automatic Flight Control*, DAR Corporation, Kansas, 2001, Chaps 1,2,3.
- [41] Talay, T.A., “Introduction To the Aerodynamics Of Flight”, *NASA SP-367*, Langley Research Center, Washington, 1975.
- [42] Chambers, J. R., “The Role of Dynamically Scaled Free-Flight Models in Support of NASA’s Aerospace Programs”, *NASA SP 2009-575*, National Aeronautics and Space Administration, Washington, 2009.
- [43] McLean, D., (1990) *Automatic Flight Control Systems*, International Series in Systems and Control Engineering by Prentice Hall.
- [44] Nise, N. S.,(2010) *Control System Engineering*, 6th ed., John Wiley & Sons, Inc.
- [45] Bandyopadhyay M. N., (2003) *Control Engineering: Theory and Practice*, Prentice-Hall of India.
- [46] Kirk, D. E., (2004) *Optimal Control Theory: An Introduction*, Dover Publications.
- [47] C2000 Piccolo LaunchPad
<http://www.ti.com/tool/LAUNCHXL-F28027>
- [48] SmartMicro Radar Altimeter
<http://www.smartmicro.de/>
- [49] Triple Axis Accelerometer & Gyro - MPU-6050
<https://www.sparkfun.com/products/11028>
- [50] Hyperion G3 CX7.4v 2S 4000mah 25C/45C Lipo
<http://www.rcdude.com/servlet/the-1644/Hyperion-G3-CX--dsh-/Detail>
- [51] Hitec HS-5645MG Metal Gear Digital Servo
<http://www.rcdude.com/servlet/the-1506/Hitec-HS-dsh-5645MG-High-Torque/Detail>
- [52] HobbyWing 40Amp OPTO Brushless Motor ESC Speed Controller
<http://www.giantshark.co.uk/product/168021/hobbywing-40amp-opto-brushless-motor-esc-speed-controller>